Studying the tumor microenvironment of Hodgkin Lymphoma with scRNA-seq

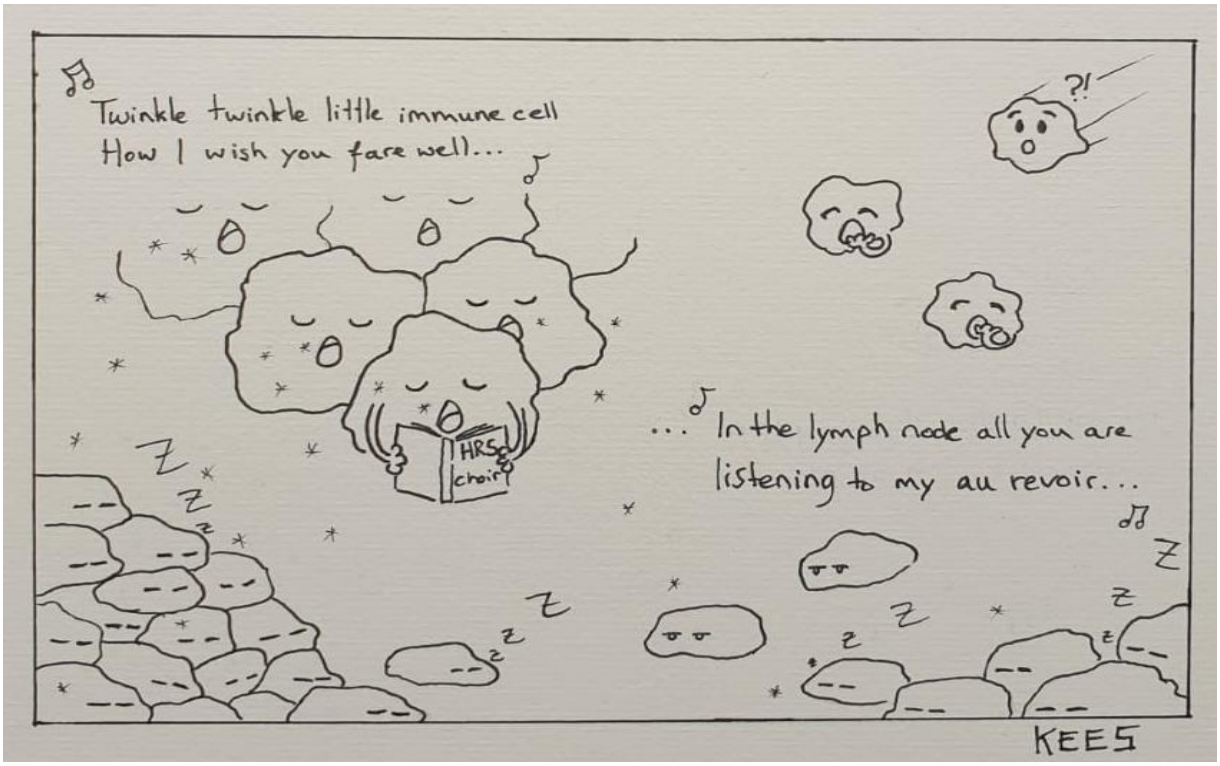

Date: 04-01-2021, 31-08-2021
Student: Kees Blijleven
Supervisor: Msc. Jurrian de Kanter
PI: dr. Ruben van Boxtel
Second examiner: dr. Patrick van Kemmeren

Table of contents

Abstract

The treatment of Hodgkin lymphoma (HL) is considered a success story: cure rates surpass 80%[1]. However, the successful treatment of HL can result in adverse side-effects later in life. Thus, there remains a need for novel therapies that result in a better quality-of-life after treatment. The tumor microenvironment (TME) affects tumor proliferation and progression. Interactions between tumor cells and their TME are being targeted as novel treatment options. A well-known inhibitory interaction in HL is PD-1 mediated inhibition of cytotoxic T-cell activity, which renders the immune system in the TME inactive and lets Hodgkin cancer cells escape immune detection[2]. To study HL TME composition in pediatric patients, samples were analysed on a single cell level. A T-cell dominant TME marked with exhaustion markers CTLA4 and LAG3 was identified. Tumor cells were identified for seven out of eight patients using a SORT-seq strategy. Interactions between tumor cells and their TME were studied with CellChat, a method that reconstructs cell-cell interaction by computing a probability score based on scRNA-seq data[3]. Finally, identified interactions were compared to previously published results. Both similarities and discrepancies were found, indicating that there is a likely biological difference between published Hodgkin protein data focussing on adults and pediatric scRNA-seq data that has been described here.

Laymen summary

Hodgkin Lymphoma is a cancer prevalent in both children and adults. The treatment success of HL is high compared to other types of cancer. However, the treatment is rough which can result in adverse effects later in life, such as infertility, cardiovascular disease and a second cancer. This is especially relevant for younger patients, since they have more time to develop these side-effects. It is not yet known whether Hodgkin Lymphoma in adults differs from Hodgkin Lymphoma in children or whether they are the exact same disease. Most conducted research focusses on adults, therefore a better characterization of Hodgkin Lymphoma in children is needed. Hodgkin Lymphoma is also a unique cancer in that there are few malignant cells present in the tumor. The majority of the tumor consists of immune cells that fail to detect and act upon the malignant tumor cells. This study aims to learn to understand how few malignant tumor cells can create an environment in which they can thrive and survive. To do so interactions between malignant tumor cells and surrounding cells in the tumor environment will be studied based on their molecular expression profiles. Each cell expresses a distinct set of molecules, some of these molecules can interact with each other. Multiple known molecular interactions will be checked to see if there are any interactions present which can explain the formation of the tumor environment. For example, an inhibitory interaction between the malignant cell and its surrounding which reduces the chance of detection by the immune system. Besides, samples from children with Hodgkin Lymphoma will be used to create a characterization of Hodgkin Lymphoma in children. Overall, both similarities and discrepancies were found with previously published results describing Hodgkin Lymphoma. The malignant tumor cells mostly behave as expected but the identified tumor environment lacks expected interactions, indicating that the Hodgkin Lymphoma environment can be diverse and might differ in children compared to adults.

Introduction

Almost 200 years ago Hodgkin lymphoma (HL) was first described by Thomas Hodgkin. It is a malignancy of the lymphoid system, which is characterized by an enlargement of lymph nodes, usually in the upper body. Each year 3 in 100.000 people are diagnosed with HL in Western countries[4]. It is the most common lymphoma among children and young adult[1]. The treatment of Hodgkin lymphoma is considered a success story: by combining several cycles of chemotherapy, radiation and alkalytic agents, cure rates surpass 80[4]. However, the successful treatment of HL results in adverse side-effects later in life. Examples include infertility[5,6], a second neoplasm[7] and increased chances of developing cardiovascular disease[8]. Some of these side-effects are more frequent in patients that receive treatment at a younger age, such as infertility. This is especially relevant for patients that receive treatment at a younger age. Thus, there is a need for novel treatments that result in a better quality-of-life after treatment. In addition, there remains a significant difference in treatment outcome between age groups in the short term after treatment, with a relatively poor outcome for older adults (>50 years)[1]. This age group has a five-year survival rate of 65% compared to 94% for pediatric patients[1]. Therefore, both adult and pediatric patients would benefit from the development of novel therapies. To be able to develop effective targeted therapies for all patient groups, a better characterization of HL is needed and the similarities and differences of adult and pediatric cases should be investigated. Currently most published literature on the molecular characterization of HL focusses on adult patients: a clear characterization of pediatric Hodgkin lymphoma is lacking.

Hodgkin lymphoma is an unusual cancer because the tumor consists of few malignant Hodgkin Reid-Sternberg cells (HRS cells, 1%) and many reactive infiltrate immune cells[4]. The HRS cells originate from germinal center B cells. In the germinal center, B cells undergo a multitude of mutations to effectively bind an antigen[9]. However, many mutations render these B cells ineffective whereupon apoptosis sets in. The HRS precursors probably evade apoptosis by some, yet unknown, rescue event. They have lost their B cell phenotype, most notably the loss of CD20 and CD79 expression and a diminishing of PAX5 expression, which might contribute to the escape of apoptosis[10]. HRS cells are characterized by high CD30, CD40 and TARC (CCL17) expression[4]. Other, more variable markers, include CD15 (FUT4), MUM1 (IRF4) and CD95 (FAS)[11,12]. Another hallmark of HRS cells is the constitutive activation of the nuclear factor kB (NF-kB) and Janus kinase STAT (JAK-STAT) signalling pathways[4]. Excessive activation of these oncogenic pathways in HL can be caused by both genetic lesions and paracrine and/or autocrine signalling[4]. This is likely one of the mechanisms with which the malignant HRS cells escape apoptosis. Besides activation of the NF-kB and JAK-STAT pathways, a multitude of other possible mechanisms have been proposed by which the HRS cells might escape immune detection. Despite the predominant presence of immune cells in the tumor there seems to be no effective immune response against the malignant HRS cells.

There is increasing evidence that tumor cells shape their tumor microenvironment (TME) via genetic alterations and altered cytokine and chemokine signalling. An example of such an interaction frequently observed in HL is the expression of PD-L1 and PD-L2 on HRS cells, usually acquired via a copy number gain or amplification on the 9th chromosome[13]. These two ligands bind the PD-1 receptor which is frequently expressed on activated T-cells, thereby

reducing their activity, proliferation and cytokine production[2]. Another regularly observed interaction is the expression of CD80 and CD86 by the HRS cells which bind the receptor CTLA4 expressed on several T-cells thereby antagonizing T-cell activation[14]. Recognition of the importance of the TME in cancer progression and treatment has led to the development and FDA approval of specific drugs targeting the tumor-TME interplay. Patients with a 9p24.1 locus gain or amplification for example responded well to the drug nivolumab, a PD-1 antibody that blocks PD-L1 from binding to PD-1 and thereby blocking PD-1 activation[15]. Refractory or relapsed patients are treated with Brentuximab Vedotin, an anti-CD30 antibody-drug conjugate which is especially effective in advanced HL stages[16]. These drugs are administered in concert with chemotherapy and often work only in a subset of patients. An increased understanding of the interactions between malignant HRS cells and their tumor microenvironment can lead to a myriad of possible targets for therapeutics in a disease with already promising cure rates.

Due to the scarcity of HRS cells in HL, studies focussing on gene expression profiles of HL have mostly used cell lines representing HL[17]. Besides altered gene expression of these cells, most studies focus on tumor cell profiling in bulk, thereby losing intratumor heterogeneity[18,19]. A better characterization of gene expression profiles of single malignant HRS cells is needed for improved disease characterization and to infer possible tumor-TME interactions which explain apoptosis and immune escape. As of yet there has been one paper published, looking into the HL TME of adult patients on a single cell level[20]. To provide a more accurate characterization of pediatric HL and HRS single cells and their interaction with the TME, samples from pediatric HL patients were analysed. First a panel with specific HRS cell markers was established to enrich tumor cells during FACS sorting. For each patient both enriched HRS cells as well as immune cells from the TME were collected after FACS sorting for single-cell RNA sequencing (scRNA-seq). Expression profiles were clustered based on similarity and assigned with cell types, including some HRS cell specific clusters. Known tumor-TME interactions from published literature were checked to confirm the Hodgkin lymphoma phenotype. Lastly, readily available R packages were used to study cell-cell interactions between the HRS cell clusters and the TME clusters, aiming to find novel interactions explaining the immune escape and tumor maintenance of pediatric Hodgkin lymphoma.

Material and Methods

SORT-seq sample preparation

Lymph nodes of HL patients (aged 14 ± 2) of the Prinses Máxima Center for pediatric oncology were surgically removed for diagnostic purposes. Single cell suspensions were made from left-over material and viably frozen. For each patient, a vial of single lymph node cells was thawed (containing 5-50 x 10^6 cells). Cells were preincubated for 5 min in FACS buffer containing 5% mouse serum and cells were kept on ice directly after thawing for the entire procedure. Of each sample, 1 x 10^6 cells were stained with 1 uM DAPI and 5 uM DRAQ5 and the rest of the cells stained with the antibody mix for 45-60 min. Antibody mix: CD20-BV421 (1:100), CD15-FITC (1:100), CD95-PE (1:100), CD30-APC (1:50), CD40-Alexa Fluor 700 (1:100), CD3-APC/Fire750 (1:100) and 0.5 uM DAPI.

Sorting cells with FACS

Following the SORT-seq protocol which combines Cel-seq2 with flow cytometry, flow cytometry-sorted single cells were deposited in 384-well plates filled with scRNA-seq reagents and primers. Per patient two 384-well plates were filled using fluorescence activated cell sorting (FACS, Sony SH800S). One plate per patient was filled with live single cells (DAPI-/DRAQ5+ singlets) and another was enriched for HRS cells. Two columns of the DAPI-/DRAQ5+ plate were filled with larger cells: SSC+, whilst all cells of the HRS plate were SSC+. For patient 25404 an extra plate of unbiased cells was analysed. Samples from patients 25404 and 26023 were enriched for tumor cells by sorting the 5% and 2% biggest cells, respectively. All other samples were enriched for HRS cells with a specific HRS cell FACS panel: DAPI-, CD20-, CD95+, CD15+, CD30+ and CD40+ for the first twelve columns of the plate. The last eleven columns were selected with the less specific HRS cell FACS panel: DAPI-, CD20-, CD95+.

Library preparation and scRNA-seq

After sorting the single cells into the 384-well plates, the plates were sent to Single Cell Discoveries, a company specialized in single-cell sequencing, for single cell RNA sequencing following the Cel-seq2 protocol[21]. In short, first reverse transcription of the RNA yielded cDNA which was pooled for in vitro transcription to amplify the RNA. After purification an Illumina sequencing library was prepared from the sample and sequenced.

Filtering and normalization

The mapping, UMI counting and other pre-processing of the data was performed with the in-house developed pipeline Sharq2[22]. Failed reactions were filtered out of the data based on the number of ERCC transcripts using the SCutils package (version 1.87). Afterwards, the scRNA-seq data was processed in R (version 4.0.3) using the Seurat package (version 4.0)[23]. Genes were filtered out of the data if there were fewer than five cells expressing the gene or if there were fewer than two transcripts of the gene in at least one cell. Count data of all cells was added to a single SeuratObject. Empty and unassigned wells were removed from the SeuratObject. Cells with few transcripts (<1000) were also removed. The count data was normalized with a natural log transformation using Seurat. For clustering and visualization cell cycle genes and sex genes were filtered out of the variable genes, they were included in further downstream analysis.

Clustering and cell typing

For clustering and visualization principal component analysis was performed using Seurat to reduce the number of dimensions and noise of the data. Out of 100 principal components the first 20 were selected based on their JackStraw score and standard deviation. The 20 components were used as input for unsupervised clustering with the shared nearest neighbour algorithm. UMAP transformation was done with the same components to visualize the clusters in UMAP space (Figure S1A). Multiple cell type classification methods were applied to the data and each cluster was manually assigned the cell type that was supported by most methods. The SingleR package (version 1.4.1)[24] was used to assign the best annotation to each cell based on a labelled reference dataset. Four bulk expression profiling databases with labelled reference cell types from the celldex package (version 1.2.0)[25] were consulted: 1) Human Primary Cell Atlas Data, 2) Blueprint Encode Data 3) Database Immune Cell Expression Data and 4) Monaco Immune Data. First more general cell types were assigned using canonical markers, resulting in four main cell types: 1) B-cells 2) T-cells, 3) myeoloid cells and 4) tumor cells. Each main cell type, except the tumor cells (see section Verify tumor cell annotation) was subsetted into a new SeuratObject and clustered again, thereby allowing for a more fine-grained clustering in which less represented (sub)types are separated better. In these new objects, SingleR was used to assign more precise cell types. For clusters with ambiguous cell typing the CHETAH package (version 1.8.0)[26] was used in addition to SingleR. This package works similarly to SingleR but assigns cell types in a hierarchical manner. Finally, known canonical markers found in published scRNA-seq papers were checked: both their expression level per cluster (Seurat VlnPlot) and their localization in UMAP space (Seurat FeaturePlot). The most common annotation found with SingleR (and CHETAH), that was in agreement with canonical marker expression, was assigned as the cell type of the cluster (Figure S1B). To verify the assigned cell types, gene ontology terms and differential expression were checked for each cluster with the clusterProfiler package (version 3.18.1)[27] and the FindMarkers function in Seurat respectively. If a newly formed cluster in the subset SeuratObject could be annotated this cluster was adopted in the complete SeuratObject. If separate clusters showed no clear difference, they were merged in the complete SeuratObject.

Verify tumor cell annotation

The reference databases used by SingleR and CHETAH do not contain HRS cells. HRS cells were annotated by SinlgeR as dendritic cells and or monocytes, indicating they have similar expression profiles. Therefore, clusters in which each patient's cells were clearly separated, were assigned as tumor cells, as tumor cells are expected to have distinct expression profiles per patient. To verify the tumor cell identity, expression of canonical HRS markers was checked (Figure S2 and S3). Genes that are generally expressed in HRS cells are CD30, CD40, CD95 (FAS), IRF4 (MUM1), CD15 (FUT4) and CCL17 (TARC). HRS cells consistently lose expression of CD20 and CD79A and have intermediate expression of PAX5. RNA expression of these markers was also compared to protein expression found by the diagnostics department of the Prinses Máxima Center (Table S1). Lastly copy number variation of the suspected HRS cells was estimated using the inferCNV package (version 1.6.0, Figure 2)[28]. inferCNV estimates copy number variation based on RNA-seq expression profiles by centering the data and subtracting the expression profile of reference cells for each corresponding gene in log-space. Gains and losses relative to the mean expression of the reference cells are visualized per chromosome in a heatmap. All T-cell clusters, NK cells, monocytes, plasmacytoid and conventional dendritic cells were used as reference cells.

iCellNet to reconstruct cell-cell interaction

iCellNet (version 0.99.1) reconstructs cell-cell interaction by computing communication scores based on co-expression of receptor-ligand pairs in transcriptomic profiles of a sender cell type (ligand expression in corresponding transcriptomes) and two receiving cell types (receptor expression in corresponding transcriptomes[29]. iCellNet uses a curated database containing 538 receptor-ligand interaction pairs including multi-subunit interactions. First, transcriptomes of both the sender and receiver cells were filtered for genes present in the iCellNet database. Then gene expression was rescaled, and a communication score was computed. This score is a product of the expression level of a specific ligand in the sender cell transcriptome and the expression of the corresponding receptor in the receiving cell its transcriptome. These individual scores are integrated into a single score representing the communication between two cell types. Note that iCellNet was used one directional (ligand to receptor) whilst it can be used to assess interaction from receptors to ligands as well. Finally, the communication score was visualized using iCellNets bubblepot.

GO term and pathway enrichment

Gene ontology (GO) terms were checked for each cell type to see if they were in accordance with the assigned cell type. GO terms were assigned based on differentially expressed genes ($p < 0.05$) using the clusterProfiler package (version3.18.1)[27]. KEGG pathway enrichment was performed using the same package to compare possibly up- and downregulated pathways between different cell types.

CellChat to reconstruct cell-cell interaction

CellChat reconstructs cell-cell interaction by computing a probability score based on differentially co-expressed receptor-ligand pairs in different cell types[3]. The default database used by CellChat contains 2,021 ligand-receptor interactions, taking both multi-subunit interactions as well as several cofactors into account. CellChat (version 1.1.0) first cross-references the ligand-receptor pairs in the scRNA-seq data and the CellChat database. Then CellChat checks for differentially expressed ligands and receptors in all cell types. To quantify interactions between cell types CellChat computes a probability value based on the law of mass action, which takes the average expression of a certain ligand in a cell type and the average expression of the corresponding receptor in another cell type. By randomly permuting cell type labels and re-assessing the communication probability the significance of an interaction between two cell types is checked. CellChat offers multiple visualization methods to aid the interpretation of the data, here the dotplot visualization was used. Since the dataset contains both abundant cell types (e.g., naive B-cells #951) and rare cell types (e.g., TFH cells #36) the communication probability was corrected for population size (computeCommunProb function from CellChat). Running CellChat was computationally intensive therefore analyses were performed using a different, smaller, database (see Database preparation for CellChat). To further restrict CellChat output ligand-receptor pairs were selected based on their pathway involvement.

Database preparation for CellChat

CellChat needs multisubunit information to run. Since the curated database from iCellNet contains a limited number of well-curated human ligand-receptor interactions and includes multisubunit information, this database was chosen. iCellNets database was formatted in Excel (Microsoft version 16.51) to meet CellChats input requirements. The database from iCellNet does not contain pathway information. To be able to filter output on pathway

involvement this information was copied from the default CellChat database for each corresponding ligand-receptor pair in the iCellNet database.

Using literature to filter HL TME interactions

To compare interactions found in the scRNA-seq data, published reviews were consulted. To find relevant reviews a search on PubMed was performed with the search key: 'hodgkin lymphoma tumor microenvironment'. Filtering for reviews and publications between 2015 and 2021, resulted in 182 papers. Reviews were then selected based on their topic: 1) they had to focus on (classical) Hodgkin Lymphoma and not another type of lymphoma and 2) the majority of the paper needed to cover the tumor microenvironment. Reviews that were not written in English were also not included. This resulted in nine reviews that were used to establish the best-known interactions found in the HL TME[30–38].

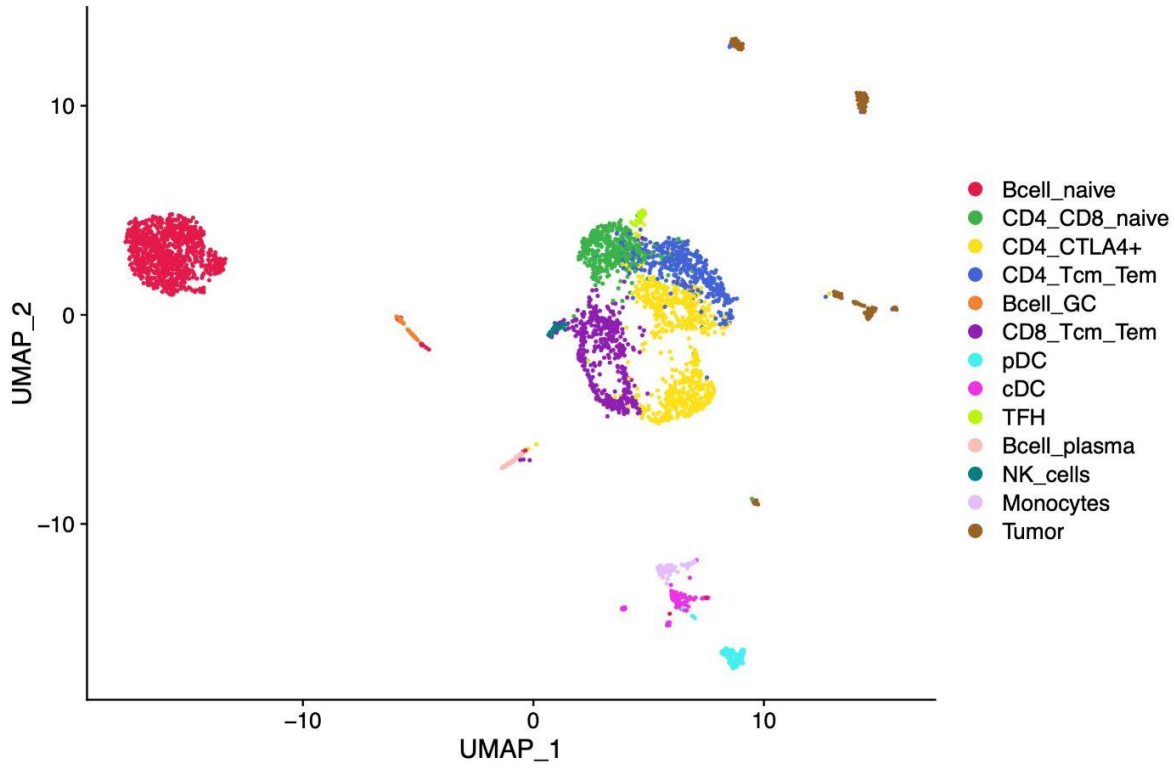

Figure 1. Single cell expression from pediatric HL in UMAP space. Pediatric HL scRNA-seq data in UMAP space, colored based on the final cell type labels. Cell types were based on unsupervised clustering on the first 20 principal components using nearest neighbour clustering from Seurat and subsequent subclustering of the four main cell types (T-cells, B-cells, tumor cells and myeloid cells).

Results

Hodgkin Lymphoma microenvironment at single cell level

To characterize the transcription profile of pediatric HL, samples from eight patients (14 ± 2 years old) were collected and processed. For each patient both live immune cells and tumor cells were sorted via Fluorescence-activated cell sorting (FACS) followed by scRNA-seq. After quality control, gene and cell filtering and normalization transcription profiles of 3625 live single cells were obtained (453 ± 130 cells per patient), with on average 2430 genes and 6978 transcripts per cell. Unsupervised clustering using Seurat identified eleven clusters in UMAP space, including three B-cell clusters, four T-cell clusters, two myeloid clusters and two tumor cell clusters. Cell types of these clusters were established using SingleR[24], a tool that assigns cell types based on known expression profiles, and scRNA-seq markers found in literature. No batch correction was performed because after such correction the tumor cells did not cluster separately but with other immune cells, making their analysis impossible. Also, cells from different patients contribute to the same clusters showing a heterogeneous spread of the cells. To assign more specific cell subtypes, all cells belonging to a single cell type, e.g., T-cells, were clustered again with only cells belonging to this cell type. Now smaller clusters could be distinguished which could be identified as separate cell types using SingleR and the canonical markers, such as Natural Killer (NK) cells and T Follicular Helper (TFH) cells (Figure S4). Some clusters were also merged for better visualization and downstream analyses based on similar expression profiles, for example the tumor cells of different patients. The cell type labels of the four subsets were merged, resulting in fourteen identified cell types in total (Figure 1).

Tumor cells were identified for seven out of eight patients (225 cells in total) although the number of tumor cells was strongly dependent on sample size and quality (28 ± 22 cells on average per patient). The tumor cells show clear CD30, CD40, CD95 and MUM-1 expression, there is variable expression of CD15 and TARC and the cells mostly lack CD20 expression, which is all in accordance with published literature (Figure S2 and S3). Expression patterns are also in accordance with the protein-based markers found by the pathology department (Table S1). Cells showing the canonical HRS markers were subjected to copy number variation (CNV) analysis using inferCNV to confirm their tumorigenic identity (Figure 2). This tool estimates chromosomal gains and losses based on RNA expression profiles using a non-malignant reference cell type, here all T-cells, NK cells, monocytes, plasmacytoid and conventional dendritic cells. Patient specific CNV patterns were obtained indicating that 1) the suspected tumor cells based on canonical markers are also identified as tumor cells based on CNV analysis and 2) the tumor cells are likely to have a clonal origin, as suspected in HL, and 3) chromosomal aberrations were unique for each tumor. To validate inferCNV's estimation, samples of another patient were whole genome sequenced and single cell RNA sequenced (Figure S5). CNV analysis of both techniques resulted in similar patterns indicating that inferCNV can make accurate chromosomal gain and loss estimations based on RNA expression profiles.

For one patient (25404) no tumor cells were identified, likely due to a difference in sorting strategy for tumor cell enrichment. Instead of sorting based on specific tumor cell markers, the first two patient samples (25404, 26023) were sorted based on cell size: the 5% and 2% biggest cells respectively. In the case of sorting the 5% biggest cells, germinal center (GC) B-

cell and TFH cells were identified. Almost no other patients contribute to these cell types, indicating that this sorting strategy could enrich for different cell types or that there is a difference in cell type composition between lymph node samples with or without HRS cells. Since HRS cells are derived from GC B-cells, this cluster could contain possible progenitor tumor cells. However, CNV analysis showed no clear gains or losses compared to the reference cell types and expression of canonical HRS markers were lacking (Figure S6).

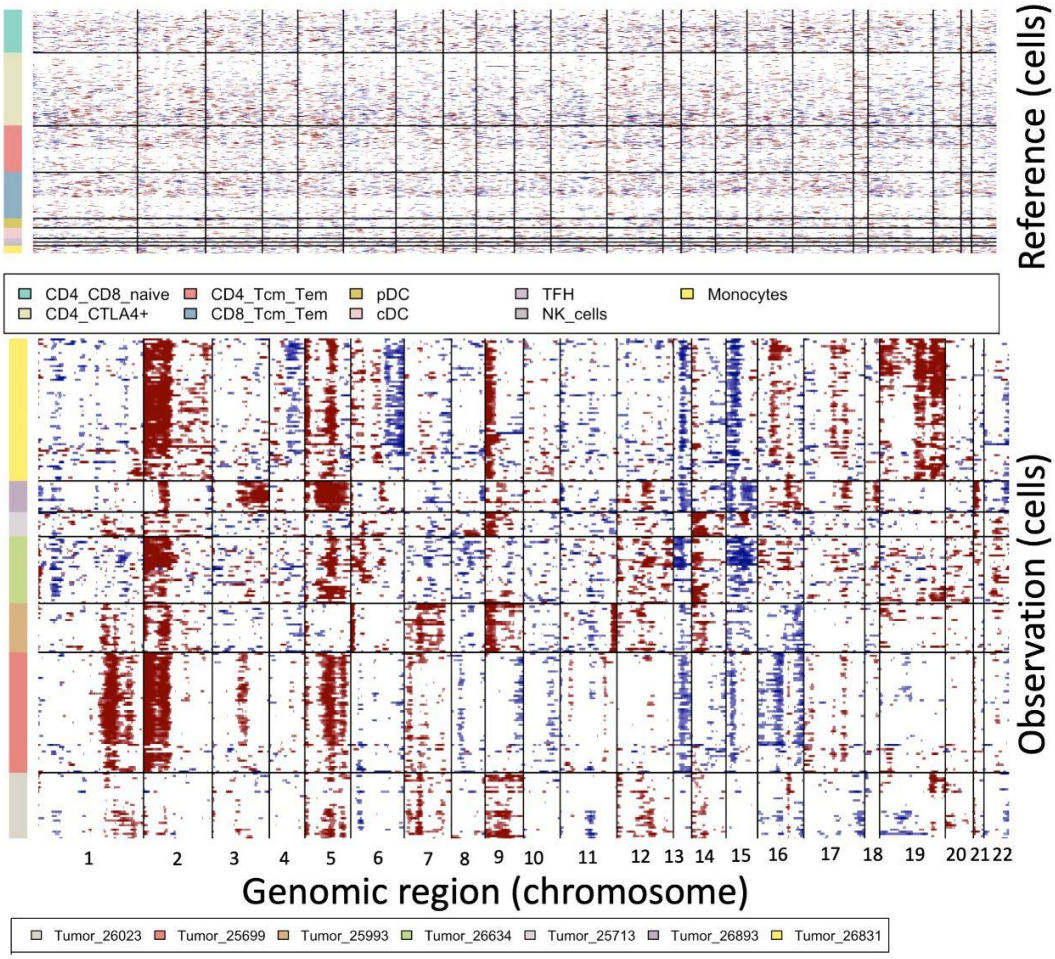

Figure 2. inferCNV analysis of HRS cells. Copy number variation, based on RNA expression, in observation cells (suspected HRS cells) have been compared to copy number variation in reference cells (T-cells, NK cells, DC cells and monocytes) using the inferCNV package.

No clear regulatory T (Treg) cell cluster was identified, while Treg involvement has often been described in HL[31,34,36]. The canonical Treg markers FOXP3 and IL2RA are expressed by some cells in the CD4 CTLA4+ cluster but not in the majority of the cells (Figure 3). Most cells do express the canonical Treg exhaustion cell marker CTLA4, hence the name of the cluster (Figure 3). Patel et al. also described a non-Treg CTLA4+ cluster in HL found by multiplexed immunofluorescence staining with a minority of FOXP3 positive cells[39]. However, Patel et al. also identify a separate FOXP3+ CTLA4- Treg population. Aoki et al. studied scRNA sequenced HL cells from adult patients and did not identify a typical FOXP3+, IL2RA+ Treg cell population as well[20]. Instead, they identified a LAG3+, CTLA4+, FOXP3- cluster, which they identify as a suppressive Treg cluster. They suggest that this is a distinct subpopulation

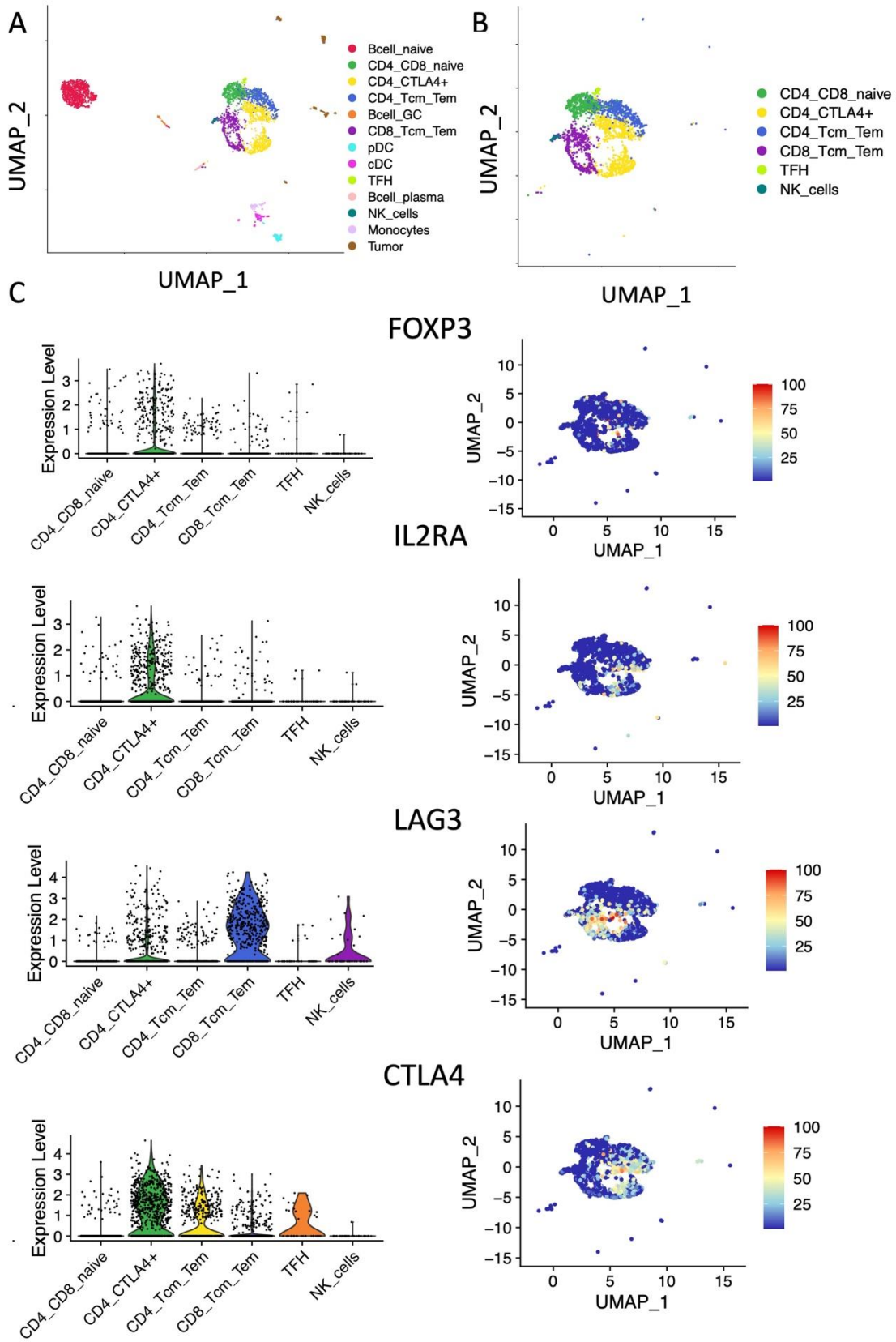

Figure 3 Marker expression in T-cells. A) Single cell expression from pediatric HL in UMAP space. **B)** T-cell subset of the dataset displayed in A. **C)** Expression of markers FOXP3, IL2RA, LAG3 and CTLA4 in the T-cell subset, shown both in a violin plot per cell type (left) and on the T-cell subset in UMAP space (right).

of CTLA4+, FOXP3- Tregs which have been described by Patel et al. The CD4+ CTLA4+ cluster identified here does not clearly express LAG3 as found in the adult HL samples (Figure 3), this seems in accordance with the CTLA4+ population described by Patel et al. However, Patel et al. do not find other inhibitory Treg markers in this population whereas the pediatric dataset presented here contains some LAG3 and FOXP3 expression in the CTLA4+ cluster.

When looking at patient specific CTLA4+ T-cells even more patient heterogeneity is discovered (Figure S7). Three patients show expression of all three exhaustion markers, FOXP3, CTLA4 and LAG3 (25404, 26023, 26634), whilst one patient expressed both FOXP3 and CTLA4 (25699). Three different patients express CTLA4 and LAG3, which is in line with the adult HL results published by Aoki et al. One patient expressed only CTLA4 (26893), as described by Patel et al. Thus, taking all samples together gives a different overview of the population composition (mostly CTLA4+FOXP3-LAG3- like Patel et al.) than looking at the markers on patient basis (most patients express at least two exhaustion markers).

CTLA4 and PD-1, two known interactions in establishing an immunosuppressive TME

Multiple interactions between HRS cells and their TME have been described that explain the immunosuppressive onset of the immune infiltrate (See Table S2 for an overview of inhibitory T-cell interactions). For example, CTLA4 which binds the ligands CD80 and CD86 which are expressed on the HRS cells (Figure S8A). Binding of CTLA4 to either ligand antagonizes T-cell activity whereas binding of CD28 to CD80 and CD86 agonizes T-cell activity[14]. CTLA4 is known to outcompete CD28, thus even at similar expression levels of CTLA4 and CD28 T-cell activity is reduced. It is a well-known and validated inhibitory interaction in HL, which makes it likely that this inhibitory interaction is taking place in these samples. Another well-known inhibitory interaction between HRS cells and their microenvironment is between the receptor PD-1, expressed on T cells, and its ligands PD-L1 and PD-L2, expressed on HRS cells[8]. Upon binding PD-1 T-cell activity is reduced. In this dataset PD-1 is expressed by TFH cells and some CD8 Tcm/Tem cells (Figure S8B). All tumor cell samples show PD-L1 expression and four out of seven patients also show PD-L2 expression. These four patients (26023, 25699, 26893, 26831) show gain of the chromosome 9 p-arm where the PD-L1/2 genes are located[13].

Using iCellNet and CellChat to study known inhibitory interactions in the HL TME

To be able to identify other novel (inhibitory) interactions between HRS cells and their microenvironment, two R packages, iCellNet and CellChat have been used. iCellNet focusses on the most different interactions between one outgoing cell type (ligand) and two incoming cell types (receptors) or vice versa, whereas CellChat compares one cell type and its most differential interactions with all other cell types (Figure 4A/C). iCellNet finds an interaction between the HRS cells (ligand, CD80, CD86) and T-cells (receptor, CTLA4) when comparing the CTLA4+ cell cluster with the TFH cell cluster (Figure 4B). According to iCellNet the CTLA4+ cell cluster has more CTLA4+-CD80/CD86 interaction with the HRS cells than the TFH cells, and this interaction is among the 30 most different interactions between CTLA4+ and TFH cells. Within the same comparison iCellNet also distinguishes the PD-L1/2 (HRS cells) interaction with PD-1 (T-cells), showing that this interaction takes place in all TFH cells but almost no CTLA4+ cells. However, neither interaction is found when comparing HRS cells (ligand) to other cell types (receptor) e.g., HRS cells interaction difference between CD4, CD8 naïve T cells and CD4 Tcm/Tem cells. Meaning that both the CTLA4 and PD-1 interaction are only among the 30 most different interactions when comparing HRS cells with CTLA4+ and TFH cells. This means that all remaining cell types have at least 30 ligand-receptor interactions

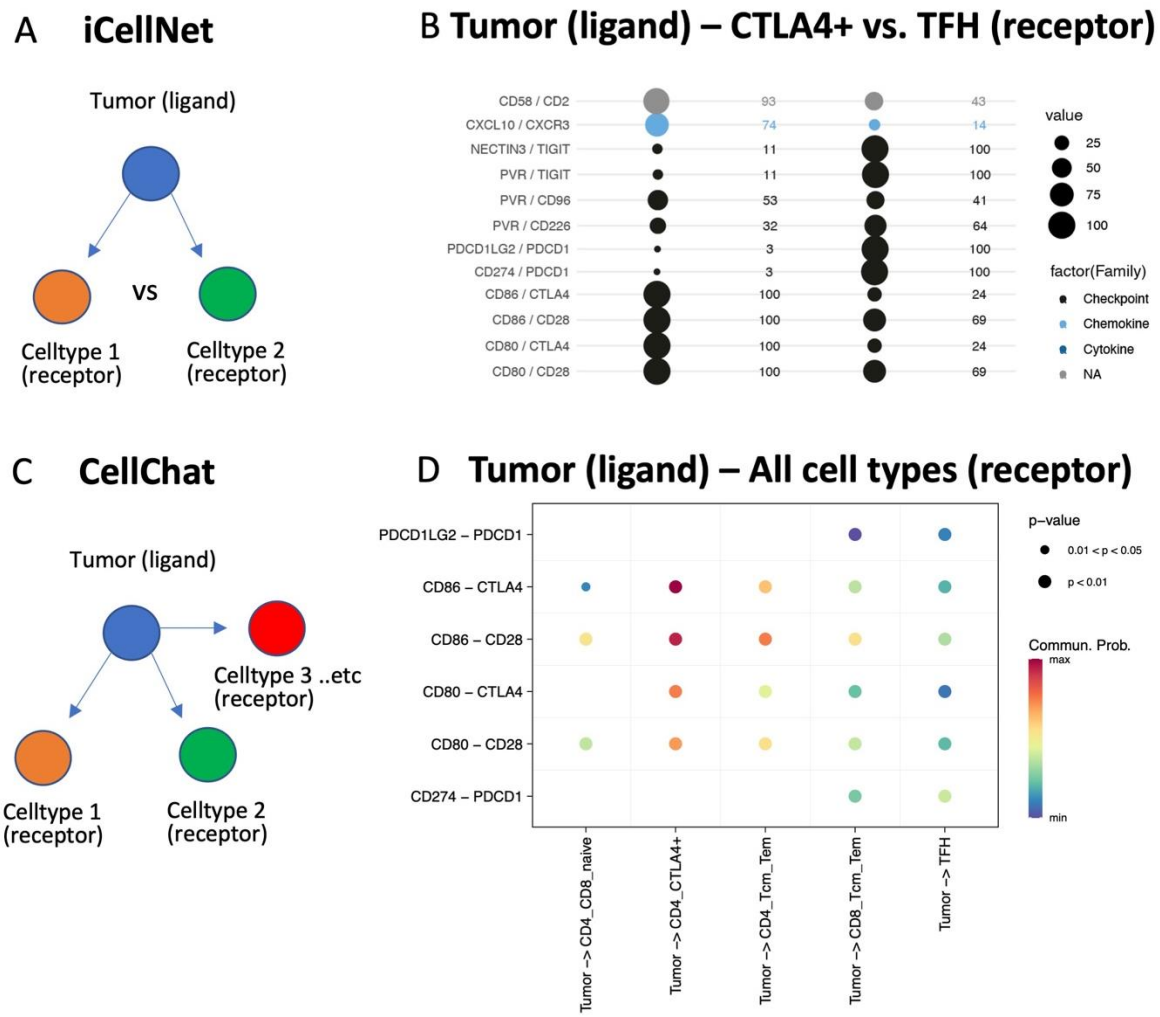

Figure 4 Methods used for cell-cell interactions. A) Schematic overview of iCellNet's operation. **B)** Bubbleplot output of iCellNet when comparing tumor (ligand, blue in A) with CTLA4+ (cell type 1 receptors, orange in A) and TFH cells (cell type 2 receptors, green in A). Plot has been shortened to 11 instead of 30 interactions. **C)** Schematic overview of CellChat's operation. **D)** Bubble plot output of CellChat when comparing tumor ligands CD80, CD86, PD-L1 (CD274) and PD-L2 (PDCD1LG2)) with receptors CTLA4, CD28 and PD-1 (PDCD1) on all other cell types.

that differ more between the cell types than the CTLA4 and PD-1 interaction: either both cell types have no CTLA4 or PD-1 interaction or the interaction level is very similar. CellChat finds interactions between HRS cells (ligand, CD80, CD86) and all T-cells (receptor, CTLA4) clusters (Figure 4D). It shows that the CTLA4-CD86 interaction between HRS cells and CTLA4+ cells are the most probable interaction followed by CTLA4-CD80. This is likely caused by the higher expression of CD86. CellChat also identifies an interaction between PD-L1/2, expressed in HRS cells, and PD-1 in both TFH cells and CD8 Tcm/Tem cells.

CellChat is able to identify and visualize all probable interactions and not the topmost different ones as iCellNet does. Thereby showing multiple interactions that are not visualized by iCellNet. Besides, CellChat provides an overview of all significant interactions between one cell type and all other cell types whereas iCellNet shows a comparison of one cell type interacting with two other cell types. Using either method to identify novel interactions without filtering led to too many interactions to manually inspect and prioritize. Therefore, known interactions found in nine published reviews were used to direct the search and filter

interactions beforehand. These interactions were subdivided into three categories: tumor driving mechanisms, mechanisms that shape the tumor microenvironment and immune escape mechanisms.

HRS cell proliferation and survival mechanisms

Germinal Center B cells with non-functional V gene mutations go into apoptosis in the germinal center. HRS precursors probably evade apoptosis by some, yet unknown, rescue event[4,9]. Once HRS cells are established there are several mechanisms which can enable their survival. HRS cells express CD30 and CD40, both members of the tumor necrosis factor receptor superfamily (TNFRSF) (Figure S9). Even in the absence of CD30 ligand (CD30L) CD30 can interact with itself and lead to activation of the NFkB pathway[40]. This effect can be enhanced by expression of CD30L but expression of CD30L is not encountered in the dataset (Figure S9). CD30 is not expressed by GC B-cells, it is likely that CD30 expression aids HRS cells in escaping apoptosis by activating the NFkB pathway. Constitutive and/or enhanced activation of NFkB is a hallmark of HL[4,41]. CD40 can also activate NFkB by binding CD40L, this ligand is expressed by CD4 Tcm/Tem and TFH cells (Figure S9). It has been shown that rosetting T-cells (CD4+ T-cells attached to HRS cells) frequently express CD40L[42]. Here some CD40L expression is seen in HRS clusters in UMAP space. There are also some T cells that show up in the HRS cluster in UMAP space. These could be rosetting T-cells that remained attached to the HRS cells during flow cytometry. Since CD40 is expressed by both GC B-cells and HRS cells (Figure S9), CD40 expression alone cannot account for apoptosis evasion. It is likely that it is the rosetting T-cells that help HRS cells escape apoptosis by expressing CD40L, thereby stimulating NFkB signalling and thus proliferation. Surprisingly KEGG pathway enrichment comparing HRS cells with GC B-cells do not show significant NFkB pathway enrichment in HRS cells (Figure S10). It does detect a significant enrichment of the JAK-STAT pathway, which is another well-known proliferative pathway with aberrant signalling in HL[4]. Several STAT factors are present in the HRS cells, e.g., STAT3, STAT5A/B and STAT6 (Figure S11A). STAT6 can be activated with autocrine signalling via IL-13 which is also expressed by HRS cells[43]. STATs can also be activated via enhanced NFkB signalling or other tyrosine kinases, of which there are many in HRS cells. Besides autocrine and paracrine stimulation of the NFkB and JAK-STAT pathways, genetic alterations are also known to cause aberrant signalling[41,44].

Receptor tyrosine kinases (RTKs) also regulate cellular proliferation, differentiation and survival. Renné et al. found that 75% of HL patients express the RTK PDGFRA whereas 30% express the RTKs DDR2, TRKA, TRKB EPHB1 and RON[45]. This is reflected in this dataset, all patients express PDGFRA whilst expression of DDR2, TRKA, TRKB, EPHB1 and RON is much more variable (Figure S11B). They found no genetic aberrations that could explain constitutive RTK activity and suggest that aberrant activity of the RTKs is likely due to autocrine (in the case of PDGFRA and EPHB1) and paracrine signalling (in the case of DDR2 and TRKA). Ligands for PDGFRA, EPHB1 and TRKA are not found in the dataset thus it remains elusive whether these RTKs are activated and if so how (Figure S11B). There is expression of collagen type 1, the ligand of DDR2, in HRS cells of the same patients which express DDR2 indicating a possible autocrine relation instead of a paracrine one as suggested by Renné et al (Figure S11B). This could also be paracrine signalling of rosetting T-cells to neighbouring HRS cells.

Shaping the HL tumor microenvironment

HRS cells secrete a plethora of cytokines that shape the HL tumor microenvironment (see Table S3 for an overview). In the dataset presented here, HRS cells express TGFβ, Galectin-1 and the immunosuppressive IL-10 which contribute to the suppression of cytotoxic T-cell activity[43,46,47]. CellChat finds significant interactions between HRS cells expressing TGFβ and IL-10 and multiple T-cell types (Figure 5). HRS cells also secrete cytokines that induce a Treg rich TME, which have an immunosuppressive effect on cytotoxic T-cells[48]. HRS cells recruit Tregs via chemoattractants such as CCL5, CCL17, and CCL2[47,49,50], which are highly expressed in all patients except 25993. T-cells in this dataset express the corresponding receptors of CCL5 (CCR5) but not the receptor of CCL17 and CCL22 (CCR4). CellChat identifies this CCL5-CCR5 interaction between HRS cells and T-cells as well (Figure 5). It also identifies other CCL interactions, most notably the CCL21-CCR7 interaction which is a known CCR7+ T-cell chemoattractant but not discussed by one of the nine HL reviews. It has been shown in cell culture that HRS cells can not only attract Tregs, but also promote the differentiation of naive CD4+ T-cells into Tregs thereby shifting even more towards a Treg dominant T-cell population[51]. T-helper cells can be polarized towards a suppressive Treg phenotype by exposure to IL-4, IL-6, IL-15 and PGE2[31,35], which are expressed in a patient dependent manner by HRS cells (Table S3). Lastly it has been shown that some HRS cells can produce IL-7 which stimulates survival and proliferation of Tregs[52]. Here only patient 26893 expresses IL-7.

As discussed, CD8 and CD4 T-cells express the T-cell exhaustion markers LAG3 and CTLA4 respectively, which signifies the dysfunction of the (cytotoxic) T-cells in the HL TME.
In this dataset PD-1 is expressed by a small part of the cytotoxic T-cells and all TFH cells. HRS cells express the corresponding ligands. Upon activation LAG3, CTLA4 and PD-1 suppress T-cell activation. This is in accordance with previously described HL that show a T-cell dominant tumor microenvironment marked by T-cell exhaustion[53]. Even though distribution of these markers differs from previously described exhausted T-cell populations. It has also been shown that CD4+ T-cells interact with HRS cells via CD40, CD80 and CD54 thereby physically protecting them from the effects of cytotoxic T-cells and NK cells[35,42].

HRS cells can stimulate the microenvironment to produce cytokines that contribute to immunosuppression, this is referred to as educating the TME (see Table S4 for an overview of educated cell types). HRS cells secrete M-CSF and or GM-CSF which stimulates monocyte differentiation into macrophages[47]. When these macrophages are exposed to TGFβ, IL-13 and MIF, also expressed by HRS cells, they can differentiate into immunosuppressive tumor associated macrophages (TAMs)[30,54]. These TAMs are CD68+ and CD163+ and can for example produce TGFβ, CCL17, CCL22, PD-L1, STAT3 and STAT6[31], thereby contributing to Treg accumulation, suppression of T-cell activity and reinstatement of HRS cells. CellChat does not identify more significant TGFβ and MIF interactions with monocytes compared to other cell types (Figure 5). In our dataset no CD68+, CD206+ macrophages were identified. There are CD68+ monocytes but they lack both CD206 and the expression of cytokines associated with TAMs. The HRS cells do express the cytokines needed for TAM induction.

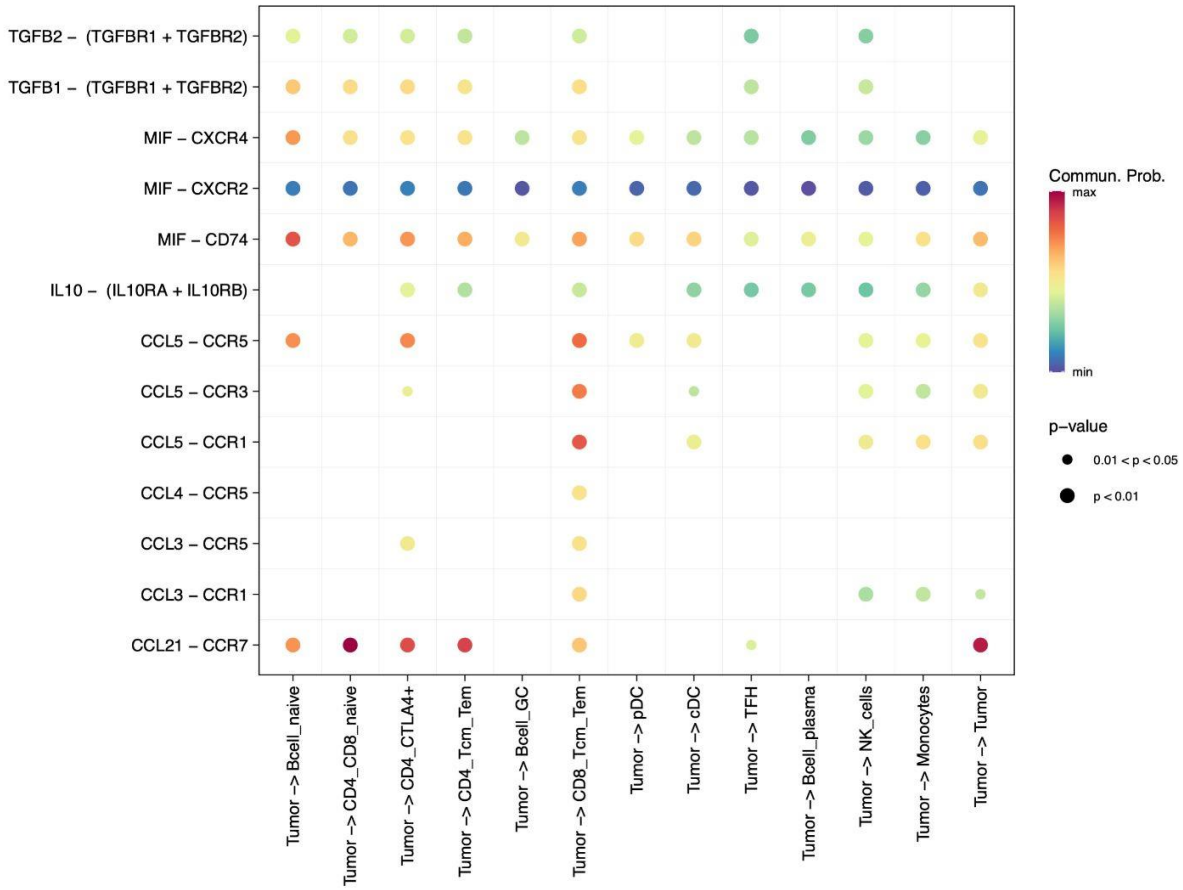

Figure 5 Cellchat interactions for TGFβ, MIF, IL-10 and CCL. Significant interactions identified by Cellchat for all TGFβ, MIF, IL-10 and CCL interactions present in the database, looking from tumor (ligand) towards all other cell types (receptor).

HRS immune escape mechanisms

HRS cells escape the immune system by establishing a protective and immunosuppressive microenvironment, but they also harbour some other mechanisms to evade immune detection (see Table S5 for an overview). A study showed that 79% (85/108) of the HL patients have reduced HLA-I protein expression on HRS cells and 67% (72/108) of the patients have reduced HLA-II expression is[55]. Surprisingly in this HL dataset there is no significant reduction of either HLA-I or HLA-II transcripts (Figure S12).

Most HRS cells have high CD95 (FAS) expression but escape FAS ligand (FASLG) induced apoptosis by overexpressing cFLIP[12]. In the presented dataset cFLIP is highly expressed by all cell types, there is no clear overexpression in HRS cells compared to other cell types (Figure S13). cFLIP inhibition of FAS-dependent apoptosis does not stop the CD95 mediated activation of the NFkB pathway, which thereby stimulates the proliferation and survival of the HRS cell instead of inducing apoptosis. It has been found that circa 30% of the HRS cells express FASLG[12]. This is not observed in this dataset, FASLG is mainly produced by NK cells and cytotoxic T-cells. In line with this, CD8 Tcm/Tem mostly interact with FAS on HRS cells (Figure 6B) according to CellChat. CellChat also identifies significant interactions between HRS cells expressing FASLG and all T-cells, most notably CTLA4+ cells (Figure 6A).

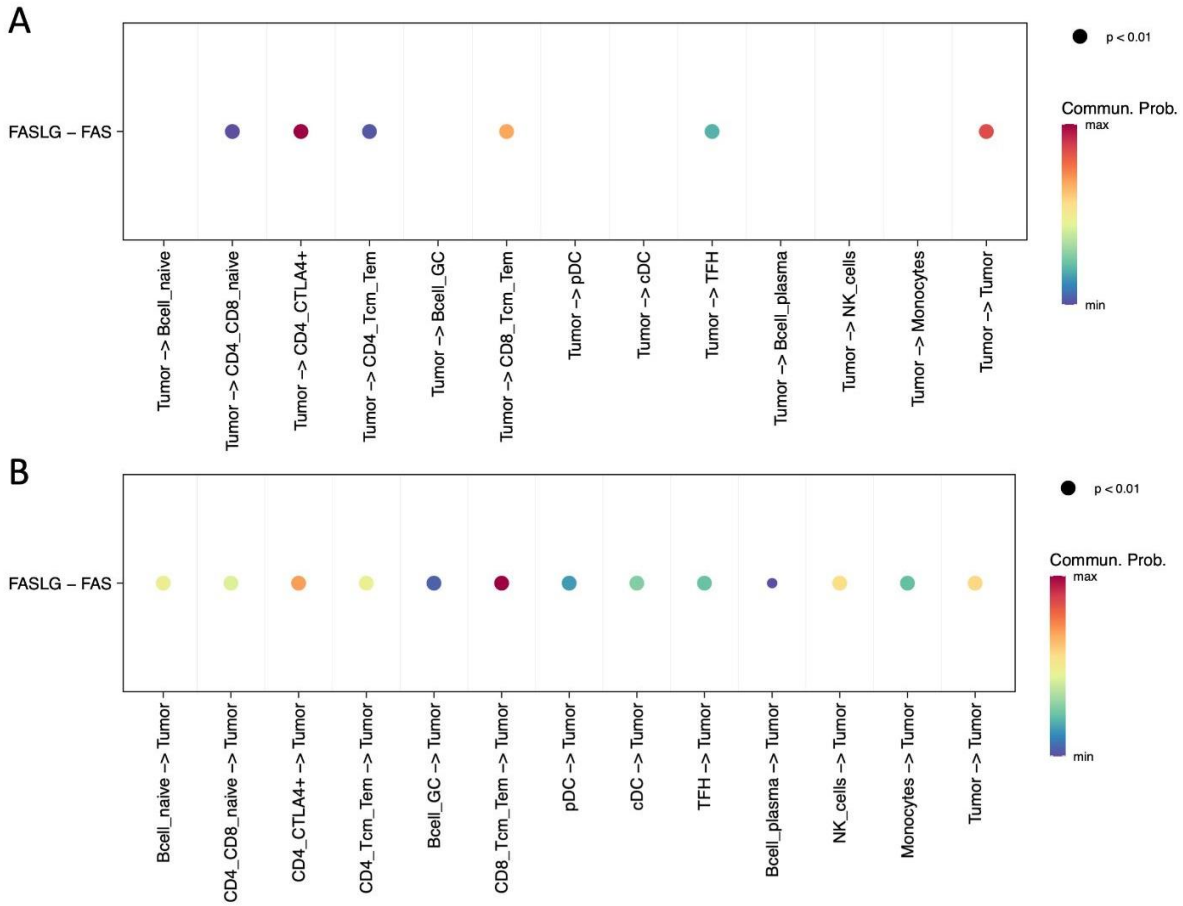

Figure 6 Cellchat interaction: FAS-FASLG. A) CellChat bubble plot visualization of HRS FASLG interaction with FAS on T-cells. **B)** CellChat bubble plot visualization FASLG expressed by the TME interaction with HRS cell FAS.

Discussion

Access to pediatric HL samples have enabled further study of HRS cells and their microenvironment at a single cell level. With the help of Seurat and CellChat, interactions between HRS cells and their TME were compared to known HL interaction. Both similarities and discrepancies have been observed and will be further discussed here.

In the unsupervised clustering of the filtered SeuratObject all tumor cells, except for tumor cells of patient 26831, were part of one cluster. This indicates that there is more difference between the expression profiles of the infiltrate immune cells than between tumor cells of different patients. Even when clustering tumor cells separately, cells did not separate based on all patient ids. This is probably due to the number of tumor cells acquired per patient. For patients 26831 and 25699, 64 and 54 HRS cells were identified respectively, and these formed clear separate clusters. Whereas for patients 25713 and 26893, 11 and 14 HRS cells were acquired respectively, and they were not separated from each other into different clusters. Because it is well known that there is inter-patient heterogeneity in tumor cells, HRS cells were labelled with patient ids even though the unsupervised clustering did not recognize them all as different clusters. This provided an easier comparison between patient differences, for example their differences in copy number variation. Both patients 25713 and 26893 have distinct CNV patterns (Figure 2). It would be valuable to check if the identified HRS cells are the same cells as selected by the HRS FACS panel.

No HRS cells were identified for patient 25404, this is possibly due to the difference in sorting strategy (5% biggest cells instead of HRS FACS panel). For patient 26023 30 HRS cells were identified when sorting the 2% biggest cells to enrich HRS cells. However, this patient was specifically selected based on their high HRS cell count. It could be that isolated cells from patient 25404 did not contain any malignant cells. Interestingly, the identified GC B-cells and TFH cells almost all belong to patient 25404. Perhaps the alternative sorting strategy enabled different cells to be sorted besides the HRS cells. However, the DAPI-DRAQ5+ plates also contained two columns with SSC+ cells (big cells) and these did not yield any GC B-cells or TFH cells, thus it seems unlikely that the difference in cell types is caused by the sorting strategy. Perhaps the tissue sample of patient 25404 does not contain HRS cells and this type of tissue does contain GC B-cells and TFH cells. inferCNV analysis of patient 25404 GC B-cells did not show any signs of aberrant CNV compared to the reference cells (Figure S6). It is therefore unlikely that these GC B-cells are progenitor HRS cells. It would be of interest to identify GC B-cells of a patient with HRS cells to compare their CNV patterns, thereby possibly identifying a progenitor HRS cell. For this purpose, GC B-cells could be enriched for with a specific FACs panel. Because a separate control tissue was lacking and because GC B-cells are recognized as the HRS cell-of-origin, GC B-cells have been used to compare HRS expression profiles. Adding scRNA-seq data of reactive lymph nodes would aid comparisons of tumor expression profiles, in addition to the intrinsic control of the immune infiltrate.

As discussed, the CTLA4+, Treg-like, population was characterized by different combinations of exhaustion markers per patient. FOXP3 and LAG3 expression were higher than anticipated when analysing the cells on a patient basis. When looking at all CTLA4+ cells, CTLA4 expression is probably dominating the lower FOXP3 and LAG3 expression, especially because the majority of the CTLA4+ cells (31%) is derived from the patient with the CTLA4+ FOXP3-LAG3- phenotype. Thus, the Treg-like cells are characterized by high expression

levels of CTLA4, and they have altering expression of FOXP3 and LAG3 per patient. Interestingly, three out of eight patients have the CTLA4+FOXP3-LAG3+ phenotype, which is described by the (only) other published scRNA-seq analysis of HL, whereas only one patient has the CTLA4+FOXP3-LAG3- phenotype as described by Patel et al. The data presented here does not support Patel et al. their assumption that HL CTLA4+ T-cells mainly express only one exhaustion marker. However, all three papers show that the T-cell population in HL is dominated by exhausted T-cells, contributing to the immunosuppressive environment of the HRS cells. This is in line with most published literature, even though a paper by Greaves et al. describes a HL TME with dominating active T-helper cells (Th1, CCR5+, TNFA+, IFNG+, IL2+)[56], showing that the T-cell population in HL can be very diverse and is not clearly understood.

In the T-cell populations no CCR4 expression was observed, even though its ligands CCL17 and CCL22 are highly expressed by the HRS cells and the interaction has been described in multiple reviews. CCR4 is mostly expressed by FOXP3+ Tregs but here the FOXP3+ T-cells do not express CCR4. This indicates that the T-cell population is not a typical Treg one.

Multiple interactions resulting in the immunosuppressive HL TME have been described. One of the most prominent examples is the PD-1 interaction with its ligand PD-L1 and PD-L2, thereby repressing T-cell activation. In this dataset PD-1 was mostly expressed by TFH cells, meaning that PD-1 expression was almost solely found in patient 25404 (Figure S8C). Consulted reviews highlight treatment with PD-1 blockade because it can be successful in patients with refractory or relapsed HL with high PD-1 ligand expression[33]. HRS cells overexpress PD-1 ligands and are frequently PD-L1+, this is in accordance with the presented data. However, there is little evidence showing PD-1 expression in the HRS TME. The same study by Greaves et al. showed that 42% of the patients had no PD-1 expression, whilst a further 40% showed PD-1 expression in less than 0.5% of their cells[56]. Thus, it could be that PD-1 blockade treatment is not successful for most HL patients but works for a specific group of patients. It could also be that PD-1 expression is induced when HL progresses due to the high PD-1 ligand exposure. Another possibility is that the difference is due to the age difference in patients, most literature describe adult HL whereas here only pediatric samples have been studied.

To further study interactions between HRS cells and their TME two R packages, iCellNet and CellChat, were used. Using the packages on their own resulted in too many different identified interactions to be interpretable. Therefore, some filter steps were incorporated. Firstly, CellChat was chosen as it provided a clearer visualization. Secondly, iCellNet's database was used because it contained fewer, well-curated ligand-receptor pairs. Finally, recent reviews were used to direct the search of interactions identified by CellChat. As a proof of concept, the CTLA4 and PD-1 interactions were checked with CellChat. CellChat indeed identified a probable interaction between these receptor-ligand pairs in the TME and HRS cells. Other interactions described in literature were also identified by CellChat, for example IL-10 expression by HRS that bind to their corresponding receptor in multiple cell types, thereby sustaining the immunosuppressive T-cell population (Figure 5). Similarly, CellChat identified TGFβ, FAS and CCL interactions between HRS cells and the TME (Figure 5). A disadvantage of using the tailored database for CellChat was that some relevant interactions could not be identified because they were not included in the database. Galectin-1 was for example for

included in the database and therefore not identified by CellChat, even though the interaction is frequently described in literature (Table S5). CellChat could benefit from a better curated database, more tailored towards interactions found in the immune system and HL TME. However, another disadvantage of this filtering approach is that no novel interactions were identified. It is more realistic to use a different method than CellChat to identify novel interaction. For example, more in-depth differential expression analysis between different cell types of interest. In this analysis it would be of interest to include data of reactive lymph nodes to aid the identification of interactions that sustain a malignant environment.

Because of the mentioned disadvantages some known interactions were not studied with Cellchat but using cell type expression profiles. Both well-known TNFSRF (e.g., CD30-CD30LG) and RTK (e.g., PDGFRA-PDGFA) ligand-receptor pairs were expressed by HRS cells and the TME. Also, high STAT expression has been observed (Figure S11A) in HRS cells and the TME, indicating stimulation of the JAK-STAT pathway. In some patients copy number gain of the 9p24.1 locus was observed, the JAK2 gene is located here besides PD-L1/2. JAK-STAT pathway enrichment was also detected by KEGG pathway enrichment analysis. Receptors, such as CD30, were highly expressed in HRS cells implying NFkB activation even though this was not detected by the KEGG pathway enrichment analysis. Aberrant signalling of JAK-STAT and NFkB are mostly caused by genomic mutations and can therefore be more accurately determined with WGS instead of single cell RNA expression profiles. Furthermore, in accordance with published literature, CD95 (FAS) was highly expressed by the HRS cells, however they do not overexpress cFLIP compared to other cell types to evade FAS induced apoptosis. HRS cells do express IL-21R which has been shown to be able to protect HRS cells from apoptosis (Table S3)[57]. Its ligand IL-21 is expressed in the HRS TME by multiple cell types. This escape mechanism has been observed in the HDLM2 cell line but could be a possible explanation for the high CD95 expression levels and the presence of (live) HRS cells.

Published results are mostly based on bulk data, whilst the results here are based on single cell data. Finding out whether cell types and global expression profiles of both methods are similar will aid the understanding of HL. Either they are similar, and the dataset can properly be compared to previously published results, or the datasets contain methodological biases, making a direct comparison more difficult. Also, most published results are based on protein expression instead of RNA expression which can explain differing expression patterns found here and described in literature. A direct comparison of the adult scRNA-seq HL data and the pediatric dataset presented here can reveal interactions not previously described by Aoki et al and might add to a better understanding of HL on a single cell level. Lastly, interactions identified with scRNA-seq need to be validated with for example immunohistochemistry staining of patient tissue samples.

Overall, both CellChat and ligand-receptor expression profiles show that HRS cells in the presented data have similar expression profiles compared to HRS cells described in published literature. There remain some discrepancies, HLA expression was for example not clearly reduced in HRS cells compared to the infiltrate, perhaps due to low FAS ligand expression levels, which normally induce HLA reduction[37]. However, there remains more ambiguity regarding the infiltrate, some cell types where not identified (e.g., macrophages and clear T helper and/or Tregs), HRS educated cell populations such as TAMs were not observed, and some well-known interactions were lacking (e.g., low PD-1 and no CCR4 expression in the

infiltrate). Since multiple papers use different patient samples and different methods to analyse HL it is no surprise that the TME compositions differs per publication. As a whole, the presented data is in accordance the predominant published results: HL consists of a T-cell rich TME, characterized by exhaustion markers and few HRS cells that have lost their typical B-cell phenotype and secrete a plethora of cytokines to create an immunosuppressive environment to aid their survival and proliferation.

References

1. Punnett, A., Tsang, R. W. & Hodgson, D. C. Hodgkin Lymphoma Across the Age Spectrum: Epidemiology, Therapy, and Late Effects. *Semin. Radiat. Oncol.* **20**, 30–44 (2010).
2. Yamamoto, R. *et al.* PD-1–PD-1 ligand interaction contributes to immunosuppressive microenvironment of Hodgkin lymphoma. *Blood* **111**, 3220–3224 (2008).
3. Jin, S. *et al.* Inference and analysis of cell-cell communication using CellChat. *Nat. Commun.* **12**, 1088 (2021).
4. Weniger, M. A. & Küppers, R. Molecular biology of Hodgkin lymphoma. *Leukemia* **35**, 968–981 (2021).
5. Howell, S. J. & Shalet, S. M. Spermatogenesis After Cancer Treatment: Damage and Recovery. *JNCI Monogr.* **2005**, 12–17 (2005).
6. Horning, S. J., Hoppe, R. T., Kaplan, H. S. & Rosenberg, S. A. Female Reproductive Potential after Treatment for Hodgkin's Disease. *http://dx.doi.org/10.1056/NEJM198106043042301* https://www.nejm.org/doi/10.1056/NEJM198106043042301 (2010) doi:10.1056/NEJM198106043042301.
7. van Leeuwen, F. E. *et al.* Long-Term Risk of Second Malignancy in Survivors of Hodgkin's Disease Treated During Adolescence or Young Adulthood. *J. Clin. Oncol.* **18**, 487–487 (2000).
8. Adams, M. J. *et al.* Cardiovascular Status in Long-Term Survivors of Hodgkin's Disease Treated With Chest Radiotherapy. *J. Clin. Oncol.* **22**, 3139–3148 (2004).
9. Marafioti, T. *et al.* Hodgkin and Reed-Sternberg cells represent an expansion of a single clone originating from a germinal center B-cell with functional immunoglobulin gene rearrangements but defective immunoglobulin transcription. *Blood* **95**, 1443–1450 (2000).
10. Adams, H., Liebisch, P., Schmid, P., Dirnhofer, S. & Tzankov, A. Diagnostic Utility of the B-cell Lineage Markers CD20, CD79a, PAX5, and CD19 in Paraffin-embedded Tissues From Lymphoid Neoplasms. *Appl. Immunohistochem. Mol. Morphol.* **17**, 96–101 (2009).
11. Tzankov, A. *et al.* Expression of B-Cell Markers in Classical Hodgkin Lymphoma: A Tissue Microarray Analysis of 330 Cases. *Mod. Pathol.* **16**, 1141–1147 (2003).
12. Metkar, S. S. *et al.* Expression of Fas and Fas Ligand in Hodgkin's Disease. *Leuk. Lymphoma* **33**, 521–530 (1999).
13. Green, M. R. *et al.* Integrative analysis reveals selective 9p24.1 amplification, increased PD-1 ligand expression, and further induction via JAK2 in nodular sclerosing Hodgkin lymphoma and primary mediastinal large B-cell lymphoma. *Blood* **116**, 3268–3277 (2010).
14. Rowshanravan, B., Halliday, N. & Sansom, D. M. CTLA-4: a moving target in immunotherapy. *Blood* **131**, 58–67 (2018).
15. Younes, A. *et al.* Nivolumab for classical Hodgkin's lymphoma after failure of both autologous stem-cell transplantation and brentuximab vedotin: a multicentre, multicohort, single-arm phase 2 trial. *Lancet Oncol.* **17**, 1283–1294 (2016).
16. Connors, J. M. *et al.* Brentuximab Vedotin with Chemotherapy for Stage III or IV Hodgkin's Lymphoma. *N. Engl. J. Med.* **378**, 331–344 (2018).

17. Devilard, E. *et al.* Gene expression profiling defines molecular subtypes of classical Hodgkin's disease. *Oncogene* **21**, 3095–3102 (2002).
18. Tiacci, E. *et al.* Analyzing primary Hodgkin and Reed-Sternberg cells to capture the molecular and cellular pathogenesis of classical Hodgkin lymphoma. *Blood* **120**, 4609–4620 (2012).
19. Steidl, C. *et al.* Gene expression profiling of microdissected Hodgkin Reed-Sternberg cells correlates with treatment outcome in classical Hodgkin lymphoma. *Blood* **120**, 3530–3540 (2012).
20. Aoki, T. *et al.* Single-Cell Transcriptome Analysis Reveals Disease-Defining T-cell Subsets in the Tumor Microenvironment of Classic Hodgkin Lymphoma. *Cancer Discov.* **10**, 406–421 (2020).
21. Hashimshony, T. *et al.* CEL-Seq2: sensitive highly-multiplexed single-cell RNA-Seq. *Genome Biol.* **17**, 77 (2016).
22. Candelli, T. *et al. Sharq, A versatile preprocessing and QC pipeline for Single Cell RNA-seq*. 250811 https://www.biorxiv.org/content/10.1101/250811v2 (2018) doi:10.1101/250811.
23. Hao, Y. *et al.* Integrated analysis of multimodal single-cell data. *bioRxiv* 2020.10.12.335331 (2020) doi:10.1101/2020.10.12.335331.
24. Aran, D. *et al.* Reference-based analysis of lung single-cell sequencing reveals a transitional profibrotic macrophage. *Nat. Immunol.* **20**, 163–172 (2019).
25. Lun, A., Andrew, J. M., Dündar, F. & Bunis, D. Pokédex for Cell Types. *Bioconductor* (2020).
26. de Kanter, J. K., Lijnzaad, P., Candelli, T., Margaritis, T. & Holstege, F. C. P. CHETAH: a selective, hierarchical cell type identification method for single-cell RNA sequencing. *Nucleic Acids Res.* **47**, e95–e95 (2019).
27. Yu, G., Wang, L.-G., Han, Y. & He, Q.-Y. clusterProfiler: an R Package for Comparing Biological Themes Among Gene Clusters. *OMICS J. Integr. Biol.* **16**, 284–287 (2012).
28. Tickle, T., Tirosh, I., Georgescu, C., Brown, M. & Haas, B. inferCNV of the Trinity CTAT Project. *Klarman Cell Obs. Broad Inst. MIT Harv. Camb. MA USA* (2019).
29. Noël, F. *et al.* Dissection of intercellular communication using the transcriptome-based framework ICELLNET. *Nat. Commun.* **12**, 1089 (2021).
30. Nagpal, P., Descalzi-Montoya, D. B. & Lodhi, N. The circuitry of the tumor microenvironment in adult and pediatric Hodgkin lymphoma: cellular composition, cytokine profile, EBV, and exosomes. *Cancer Rep.* **4**, e1311 (2021).
31. Aldinucci, D., Borghese, C. & Casagrande, N. Formation of the Immunosuppressive Microenvironment of Classic Hodgkin Lymphoma and Therapeutic Approaches to Counter It. *Int. J. Mol. Sci.* **20**, 2416 (2019).
32. Calabretta, E., d'Amore, F. & Carlo-Stella, C. Immune and Inflammatory Cells of the Tumor Microenvironment Represent Novel Therapeutic Targets in Classical Hodgkin Lymphoma. *Int. J. Mol. Sci.* **20**, 5503 (2019).
33. Liu, W. R. & Shipp, M. A. Signaling pathways and immune evasion mechanisms in classical Hodgkin lymphoma. *Hematol. Am. Soc. Hematol. Educ. Program* **2017**, 310–316 (2017).
34. Vardhana, S. & Younes, A. The immune microenvironment in Hodgkin lymphoma: T cells, B cells, and immune checkpoints. *Haematologica* **101**, 794–802 (2016).
35. Aldinucci, D., Celegato, M. & Casagrande, N. Microenvironmental interactions in classical Hodgkin lymphoma and their role in promoting tumor growth, immune escape and drug resistance. *Cancer Lett.* **380**, 243–252 (2016).
36. Wein, F. & Küppers, R. The role of T cells in the microenvironment of Hodgkin lymphoma. *J. Leukoc. Biol.* **99**, 45–50 (2016).
37. Carbone, A., Gloghini, A., Castagna, L., Santoro, A. & Carlo-Stella, C. Primary refractory and early-relapsed Hodgkin's lymphoma: strategies for therapeutic targeting based on the tumour microenvironment. *J. Pathol.* **237**, 4–13 (2015).
38. Carlo-Stella, C. & Santoro, A. Microenvironment-related biomarkers and novel targets in classical Hodgkin's lymphoma. *Biomark. Med.* **9**, 807–818 (2015).

39. Patel, S. S. *et al.* The microenvironmental niche in classic Hodgkin lymphoma is enriched for CTLA-4–positive T cells that are PD-1–negative. *Blood* **134**, 2059–2069 (2019).
40. Horie, R. *et al.* Ligand-independent signaling by overexpressed CD30 drives NF-κB activation in Hodgkin–Reed-Sternberg cells. *Oncogene* **21**, 2493–2503 (2002).
41. Weniger, M. A. & Küppers, R. NF-κB deregulation in Hodgkin lymphoma. *Semin. Cancer Biol.* **39**, 32–39 (2016).
42. Carbone, A. *et al.* Expression of Functional CD40 Antigen on Reed-Sternberg Cells and Hodgkin's Disease Cell Lines. *Blood* **85**, 780–789 (1995).
43. Kapp, U. *et al.* Interleukin 13 Is Secreted by and Stimulates the Growth of Hodgkin and Reed-Sternberg Cells. *J. Exp. Med.* **189**, 1939–1946 (1999).
44. Tiacci, E. *et al.* Pervasive mutations of JAK-STAT pathway genes in classical Hodgkin lymphoma. *Blood* **131**, 2454–2465 (2018).
45. Renné, C., Willenbrock, K., Küppers, R., Hansmann, M.-L. & Bräuninger, A. Autocrine- and paracrine-activated receptor tyrosine kinases in classic Hodgkin lymphoma. *Blood* **105**, 4051–4059 (2005).
46. Juszczynski, P. *et al.* The AP1-dependent secretion of galectin-1 by Reed–Sternberg cells fosters immune privilege in classical Hodgkin lymphoma. *Proc. Natl. Acad. Sci. U. S. A.* **104**, 13134–13139 (2007).
47. Skinnider, B. F. & Mak, T. W. The role of cytokines in classical Hodgkin lymphoma. *Blood* **99**, 4283–4297 (2002).
48. Marshall, N. A. *et al.* Immunosuppressive regulatory T cells are abundant in the reactive lymphocytes of Hodgkin lymphoma. *Blood* **103**, 1755–1762 (2004).
49. van den Berg, A., Visser, L. & Poppema, S. High Expression of the CC Chemokine TARC in Reed-Sternberg Cells. *Am. J. Pathol.* **154**, 1685–1691 (1999).
50. Aldinucci, D. *et al.* Expression of CCR5 receptors on Reed–Sternberg cells and Hodgkin lymphoma cell lines: Involvement of CCL5/Rantes in tumor cell growth and microenvironmental interactions. *Int. J. Cancer* **122**, 769–776 (2008).
51. Tanijiri, T. *et al.* Hodgkin's Reed-Sternberg cell line (KM-H2) promotes a bidirectional differentiation of CD4+CD25+Foxp3+ T cells and CD4+ cytotoxic T lymphocytes from CD4+ naive T cells. *J. Leukoc. Biol.* **82**, 576–584 (2007).
52. Cattaruzza, L. *et al.* Functional coexpression of Interleukin (IL)-7 and its receptor (IL-7R) on Hodgkin and Reed-Sternberg cells: Involvement of IL-7 in tumor cell growth and microenvironmental interactions of Hodgkin's lymphoma. *Int. J. Cancer* **125**, 1092–1101 (2009).
53. Jiang, Y., Li, Y. & Zhu, B. T-cell exhaustion in the tumor microenvironment. *Cell Death Dis.* **6**, e1792–e1792 (2015).
54. Yaddanapudi, K. *et al.* Control of tumor-associated macrophage alternative activation by MIF. *J. Immunol. Baltim. Md 1950* **190**, 2984–2993 (2013).
55. Roemer, M. G. M. *et al.* Classical Hodgkin Lymphoma with Reduced β2M/MHC Class I Expression is Associated with Inferior Outcome Independent of 9p24.1 Status. *Cancer Immunol. Res.* **4**, 910–916 (2016).
56. Greaves, P. *et al.* Defining characteristics of classical Hodgkin lymphoma microenvironment T-helper cells. *Blood* **122**, 2856–2863 (2013).
57. Lamprecht, B. *et al.* Aberrant expression of the Th2 cytokine IL-21 in Hodgkin lymphoma cells regulates STAT3 signaling and attracts Treg cells via regulation of MIP-3α. *Blood* **112**, 3339–3347 (2008).

Supplementary figures

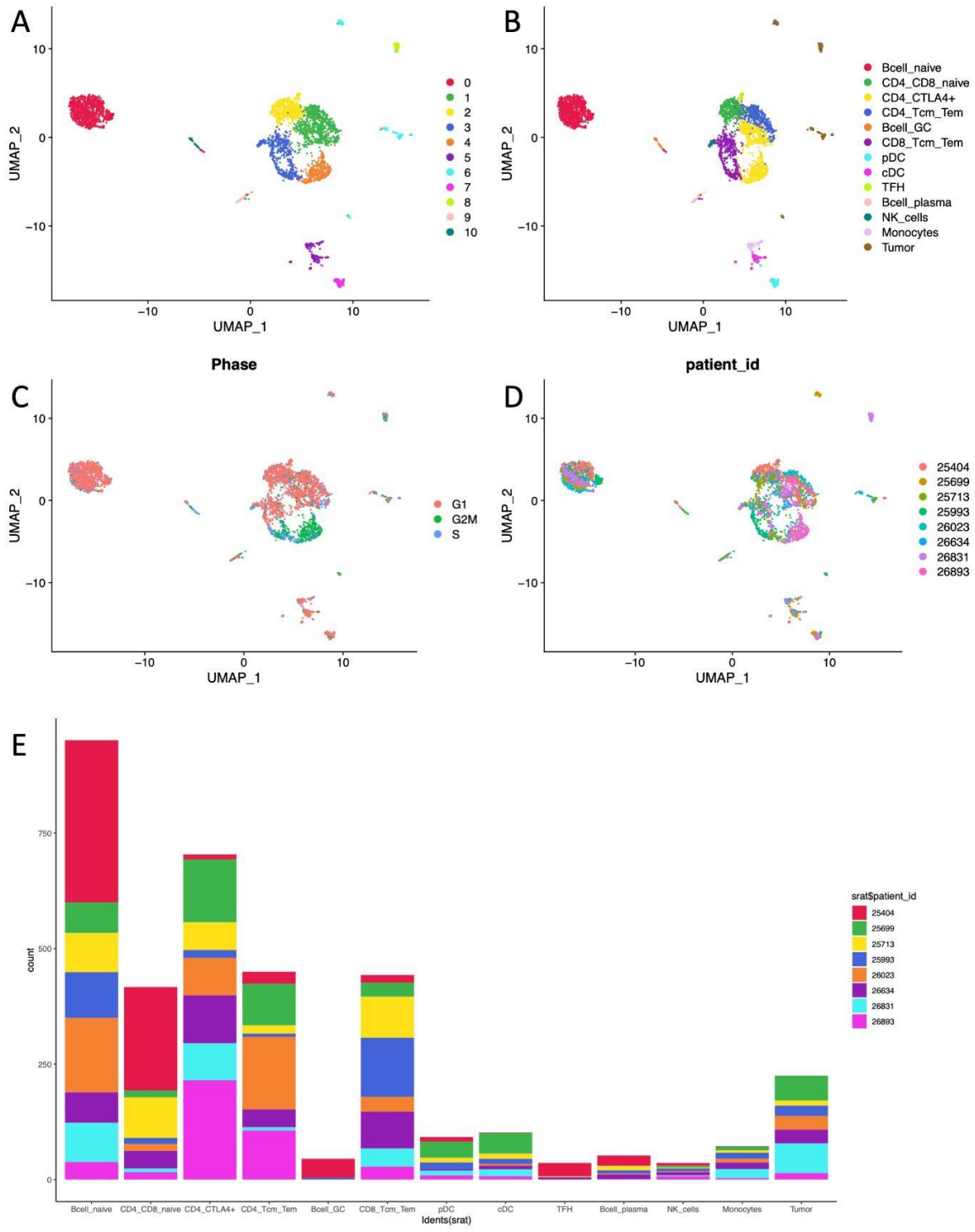

Figure S1. Clustering of the count data. A) Unsupervised clustering of the 20 first principal components of the count data visualized in UMAP space. **B)** Clusters after assigning cell types. **C)** Cell cycle phase of each cell mapped onto the UMAP clusters. **D)** Patient id's of each cell mapped onto the UMAP clusters. **E)** Barplot with patient contribution per cluster.

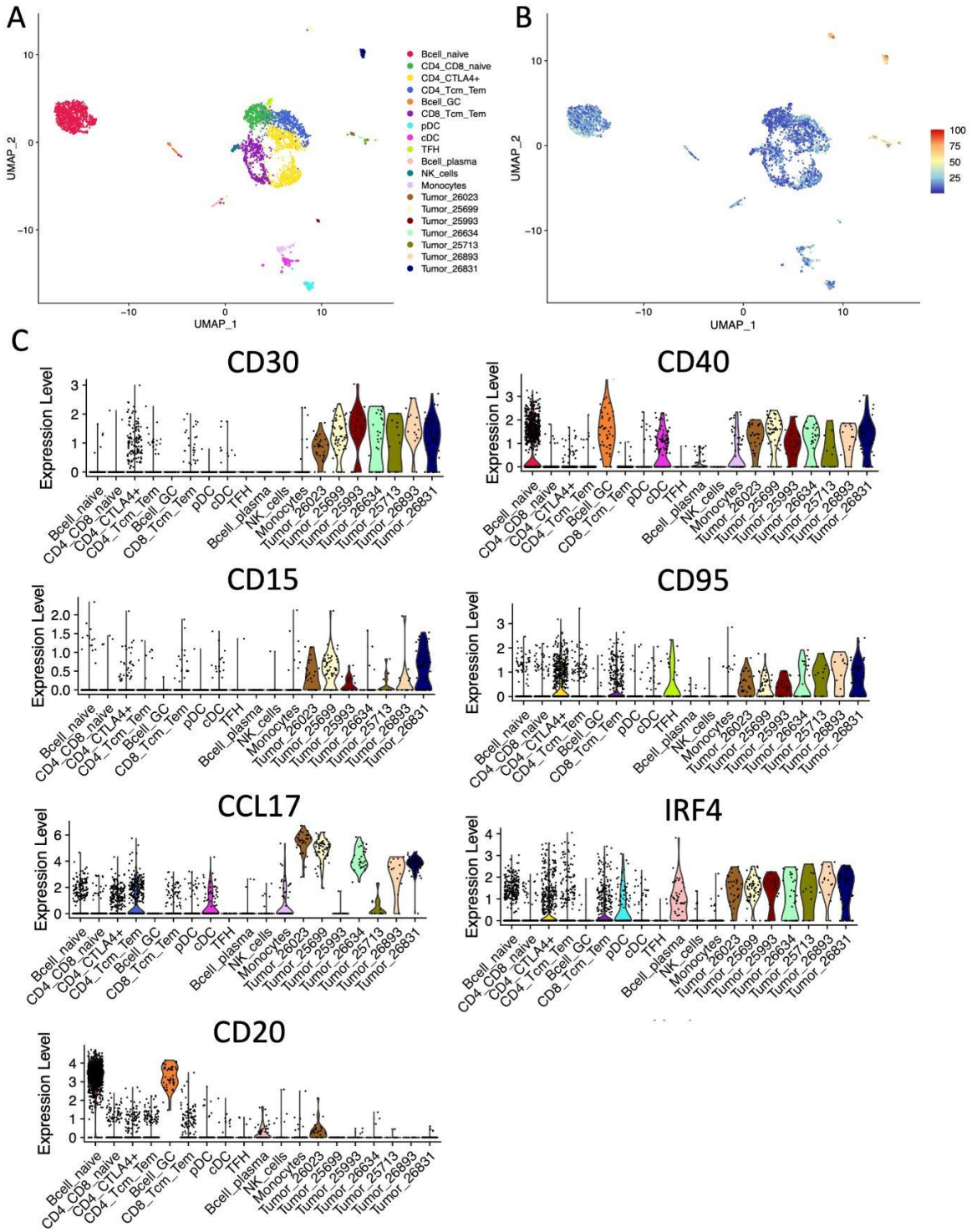

Figure S2. Canonical HRS cell marker expression. A) Single cell expression from pediatric HL in UMAP space. **B)** UMAP plot where each cell is colored with its HRS module score. A module score shows the average expression of a given set of markers compared to a random set of markers. Here the HRS markers CD30, CD40, CD15, CD95, CCL17 and IRF4 have been used to calculate the module score. There is on average more expression of these markers in the red cells compared to the blue cells, indicating that they are HRS cells. **C)** Violin plots of all canonical HRS markers mentioned in B plus CD20, which is absent in HRS cells. The number of HRS cells per patients identified: 25404: 0, 25699: 54, 25993: 22, 26023: 30, 25713: 11, 26634: 30, 26893: 14, 26831: 64.

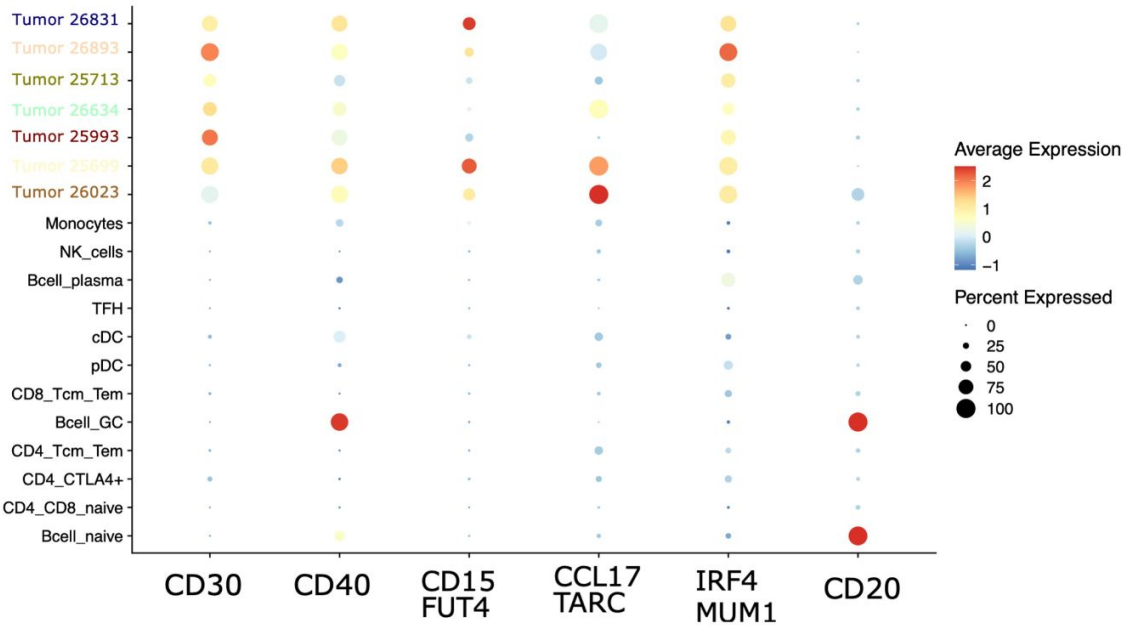

Figure S3. Dotplot of canonical HRS cell marker expression. Alternative visualization of figure S2C. Showing the average expression of canonical HRS cell markers compared to all other cell types.

Table S1. Diagnostics HRS cell marker comparison. The RNA tables show expression levels found in scRNA-seq of HRS cells: +) high expression +/-) moderate expression -) no expression. The IHC (immunohistochemistry) tables show expression levels found on HRS cells by the diagnostics department using the same legend. In red differing outcomes have been highlighted.

PatientID →	26023		25699		25993		26634		25713		26893		26831	
Marker ↓	RNA	IHC	RNA	IHC	RNA	IHC	RNA	IHC	RNA	IHC	RNA	IHC	RNA	IHC
CD30	+	+	+	+	+	+	+	+	+	+	+	+	+	+
CD20	+/-	-	-	-	-	-	-	-	-	-	-	-	-	-
CD15/FUT4	+	+	+	+	+/-	+/-	-	+	+/-	+	+/-	+/-	+	+
PAX5	+	+	+/-	+/-	+	+	-	+	+	+	+/-	+	+	+
CD79A	+/-	-	-	-	-	-	-	-	-	-	-	-	-	-
MUM1/IRF4	+	+	+	+	+	+	+	+	+	+	+	+	+	+
TARC/CCL17	+	+	+	+	-	-	+	+	+/-	+/-	+	+	+	+
ALK	-	-	-	-	-	-	-	-	-	-	-	-	-	-

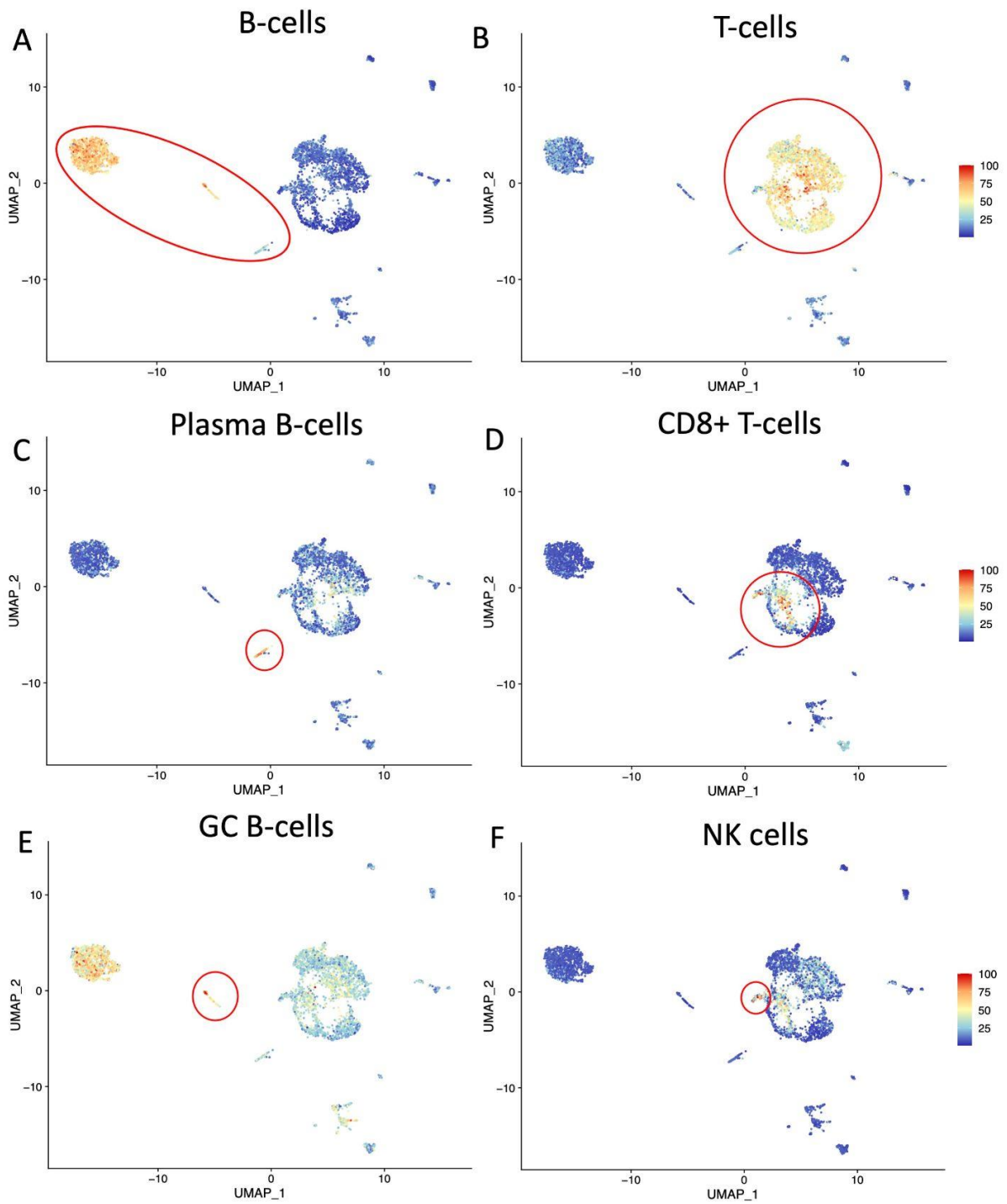

Figure S4A-F. Module scores of all non-tumor cell types. UMAP plots where each cell is colored with its respective module score. A module score shows the average expression of a given set of markers compared to a random set of markers. **A)** B-cell markers used: CD19, CD20, CD79A, CD79B, BLNK. **B)** T-cell markers used: CD2, CD3D, CD3E, CD3G. **C)** Plasma B-cell markers used: SDC1, TNFRSF17, PRDM1, XBP1, FKBP11. **D)** CD8 T-cell markers used: CD8, GZMA, GZMB, GZMH, GZMK, PRF1. **E)** Germinal center B-cell markers used: PTPRC, CD27, CD19, CD40, CD38, CD83, CIITA. **F)** NK cell markers used: CD3, NCAM1, CD16, GZMA, KIR2DL1, KIR2DL3, FASLG, KLRB1.

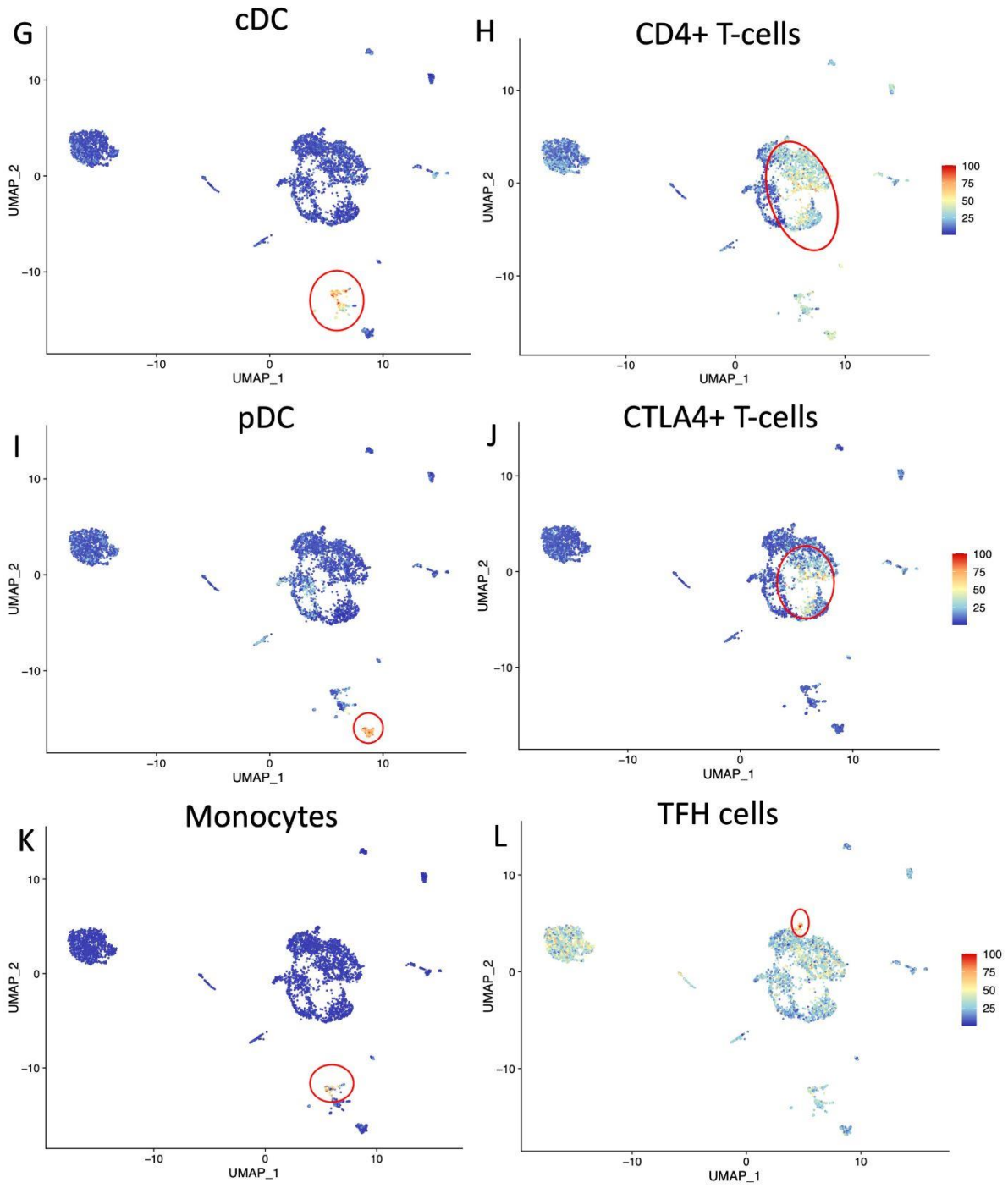

Figure S4G-L. Modulescores of all non-tumor cell types. UMAP plots where each cell is colored with its respective module score. A module score shows the average expression of a given set of markers compared to a random set of markers. **G)** conventional dendritic cell markers used: SERPINA1, LST1, AIF1, S100A9, LYZ, CLEC10A. **H)** CD4 T-cell markers used: CD4, FOXP3, IL2RA. **I)** Plasmacytoid dendritic markers used: GZMB, IL3RA, SERPINF1, ITM2C. **J)** CTLA4 T-cell markers used: CTLA4, FOXP3, IL2RA. **K)** Monocyte markers used: CD14, S100A8, S100A9, FCN1, CSF3R. **L)** T follicular helper cell markers used: IL6ST, TOX, CD200, SLAMF6, RILPL2, PLEKOH1, IL-4, LIF, CXCR5, BCL6.

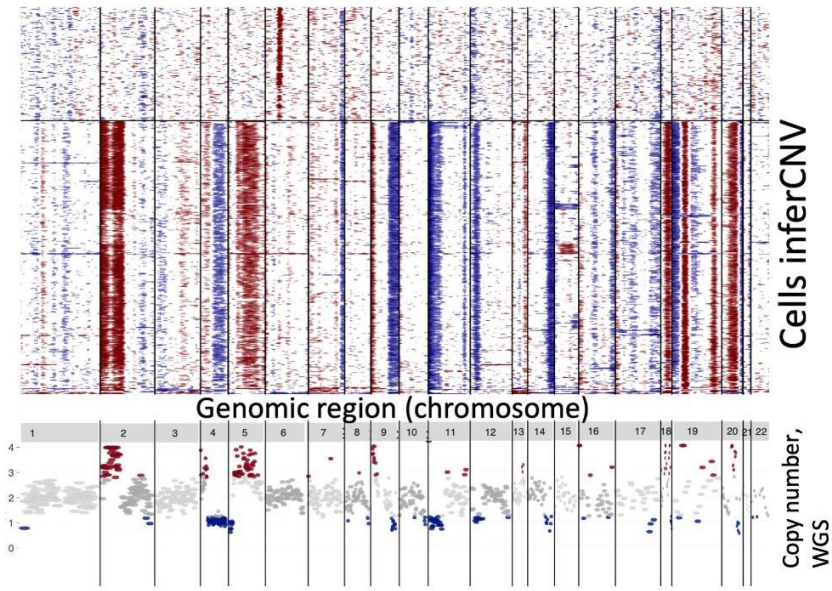

Figure S5. inferCNV and WGS of one HL patient. To validate inferCNV HL cells of one patient were scRNA sequenced and analysed with inferCNV and compared to CNV found after whole genome sequencing (WGS). Red indicates a copy number gain and blue a copy number loss.

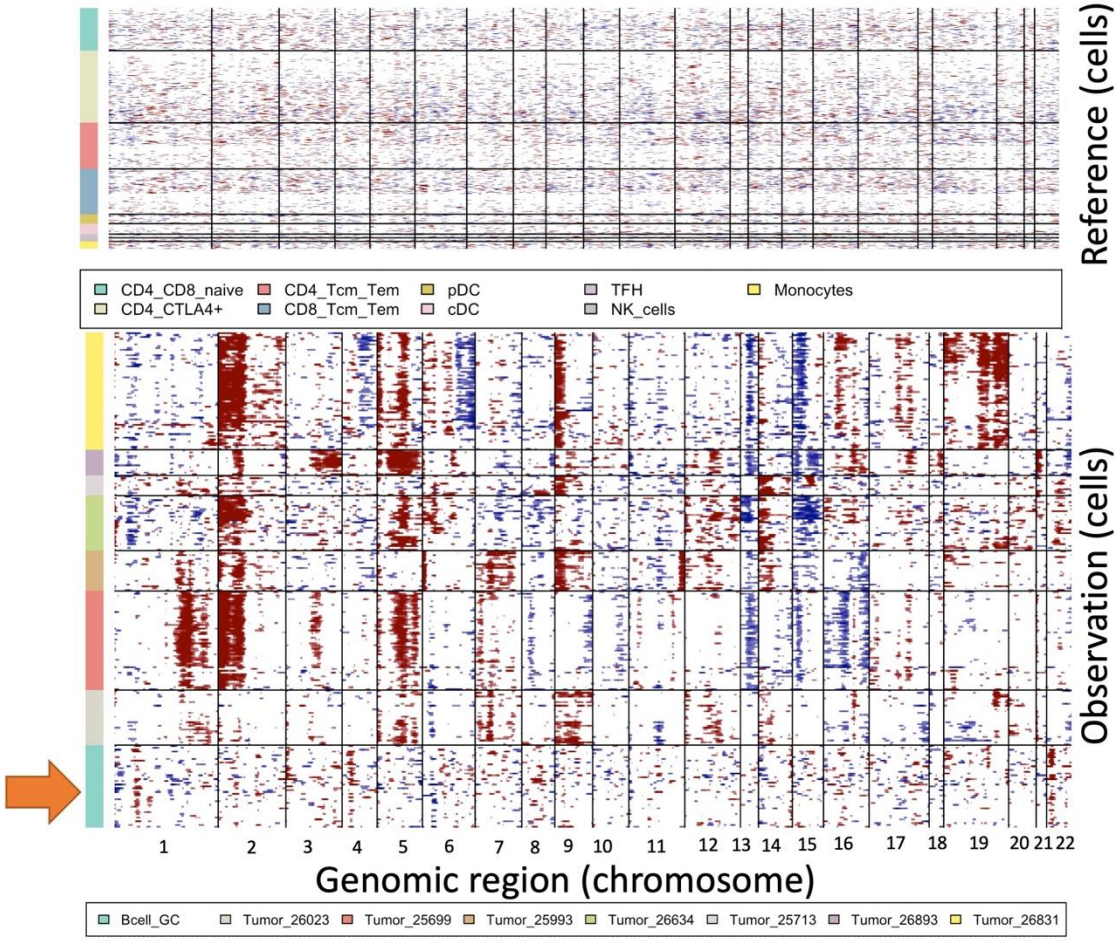

Figure S6. inferCNV analysis of HRS cells and GC B-cells. Copy number variation, based on RNA expression, from observation cells (suspected HRS cells and GC B-cells (orange arrow)) have been compared to copy number variation in reference cells (T-cells, NK cells, DC cells and monocytes).

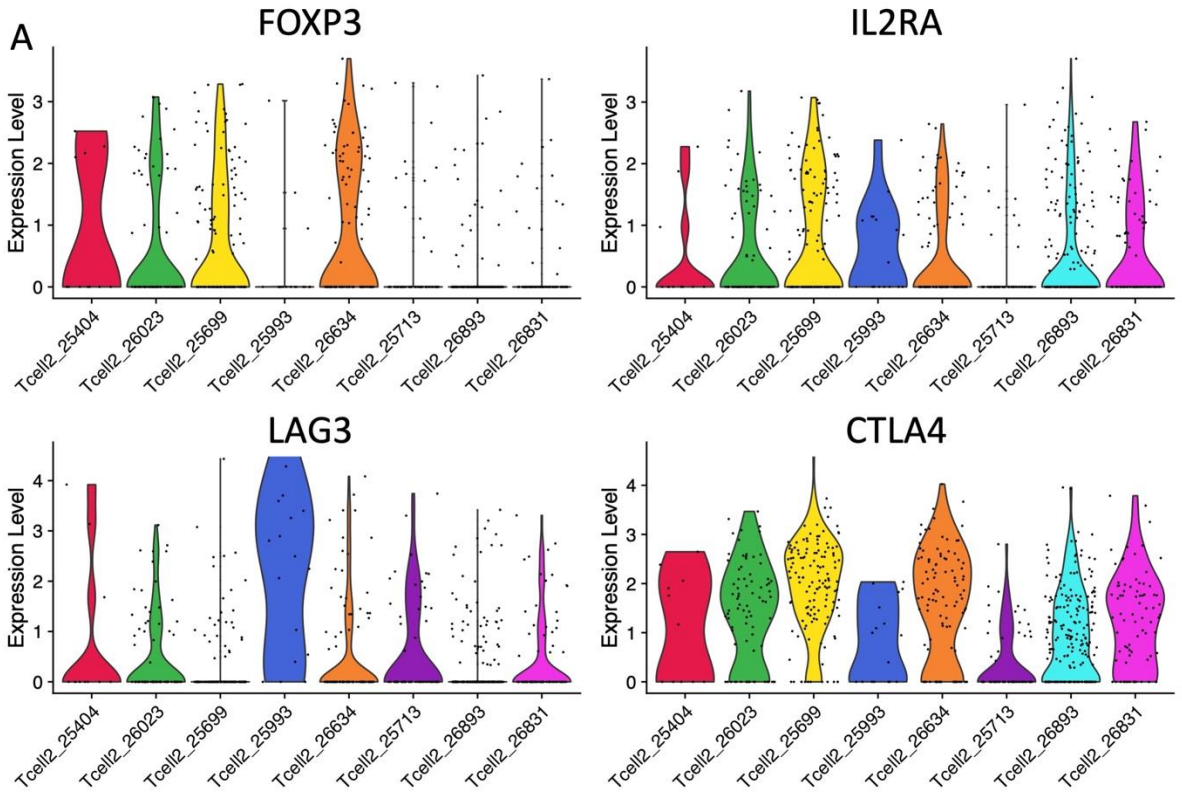

B

Phenotype	Patient ID
CTLA4+, FOXP3-, LAG3-	26893
CTLA4+, FOXP3+, LAG3-	25699
CTLA4+, FOXP3-, LAG3+	25713, 25993, 26831
CTLA4+, FOXP3+, LAG3+	25404, 26023, 26634

Figure S7. Treg marker expression in CTLA4+ cell type per patient. A) CTLA4+ cells have been visualized per patient showing patient specific expression of the Treg marker IL2RA and the three Treg exhaustion markers FOXP3, LAG3 and CTLA4. **B)** dominating CTLA4+ cell phenotype per patient.

Table S2. Inhibitory interactions between HRS cells and T-cells. Summary of inhibitory interactions between HRS cells and T-cells in their TME, described by the nine reviews used to establish a current understanding of the HL TME. The PD-1 interaction has been described by all nine reviews whereas the other interactions described less frequently.

Inhibitory T-cell interactions	expressed by HRS	expressed by TME	Review
HRS cells supress T-cell activity by activating inhibitory receptors	PD-L1/L2 CD80/CD86 N/A	PD-1 CTLA4 LAG3	30-38 31,34 34
HRS cells supress T-cell activity by competing for the ligand in the TME	CD137 CD200 HVEM	CD137LG CD200R BTLA	31,35,36 31 31

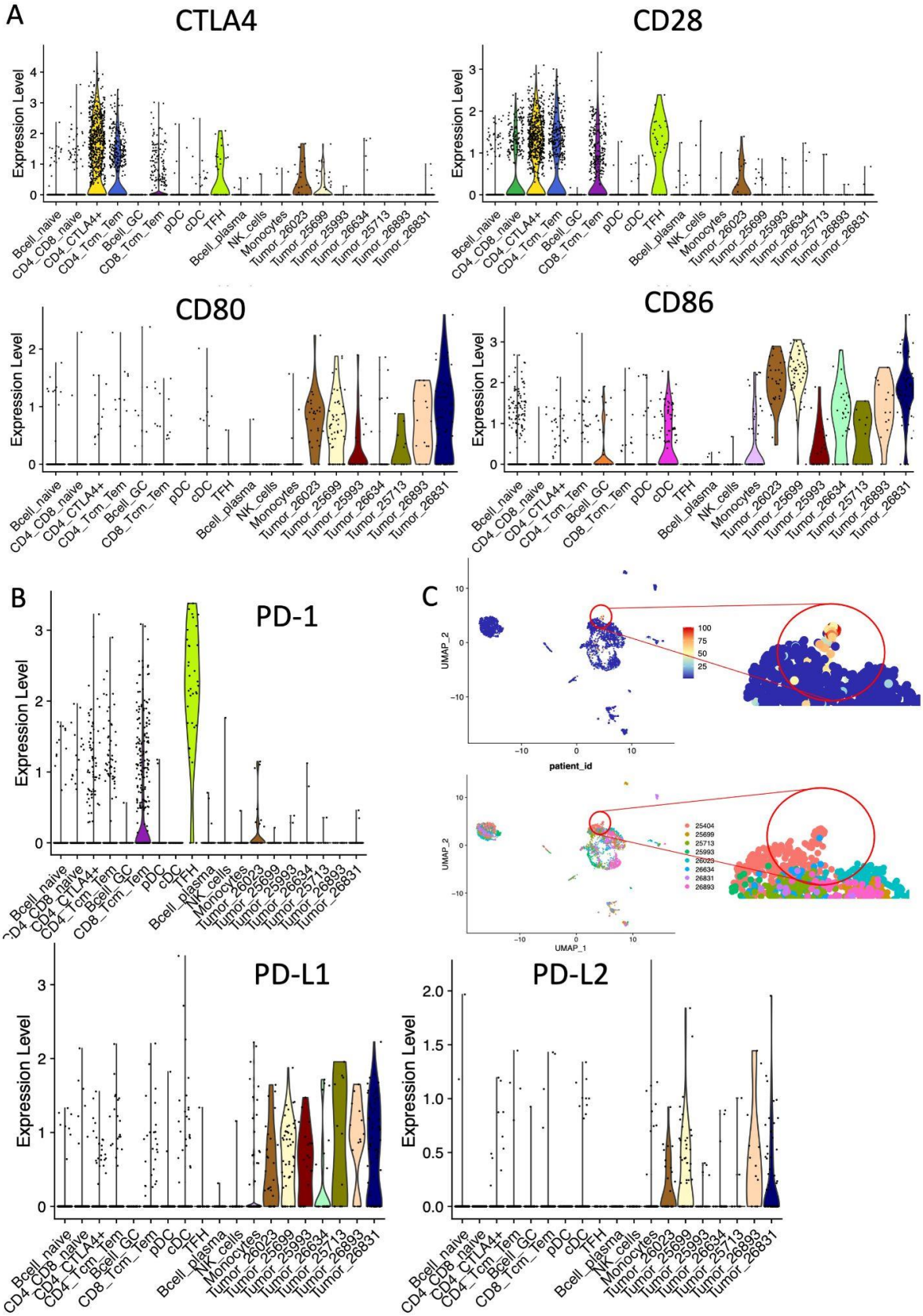

Figure S8 Inhibitory interactions in HL. A) Expression of receptors CTLA4 and CD28 and their corresponding ligands CD80 and CD86. **B)** Expression of PD-1 and its ligands PD-L1 and PD-L2. **C)** UMAP plots of PD-1 expression and patient IDs, cells that express PD-1 mostly belong to patient 25404.

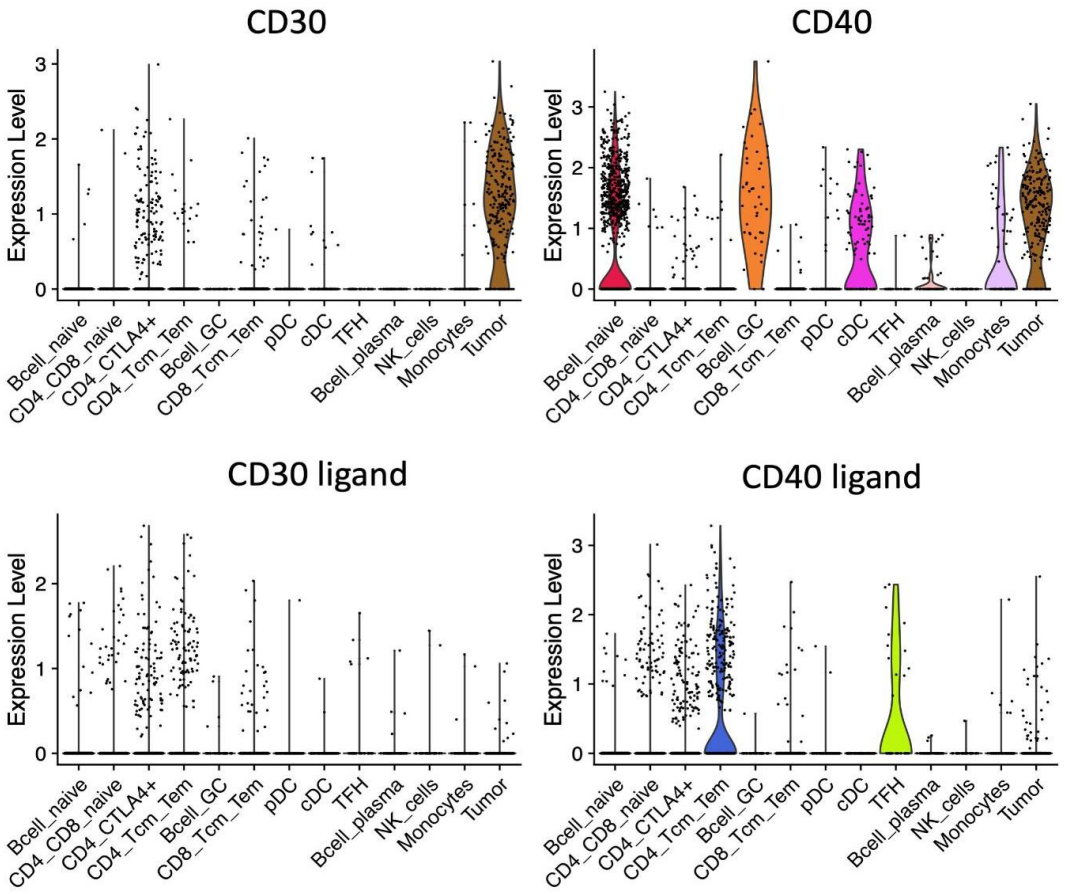

Figure S9 Expression of some TNFSFs. High CD30 and CD40 expression is observed in tumor cells. The HRS TME expresses CD40 ligand and little CD30 ligand.

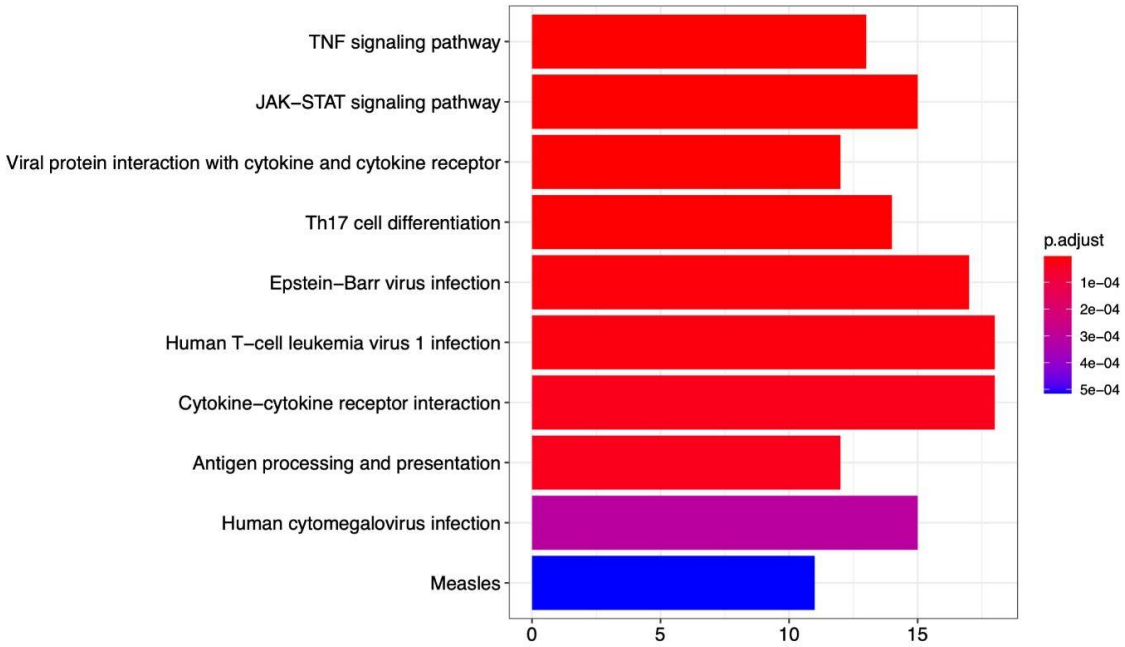

Figure S10 KEGG pathway enrichment HRS cells vs. GC B-cells. Most significantly enriched pathways in HRS cells compared to GC B-cells, based on genes that are differentially expressed.

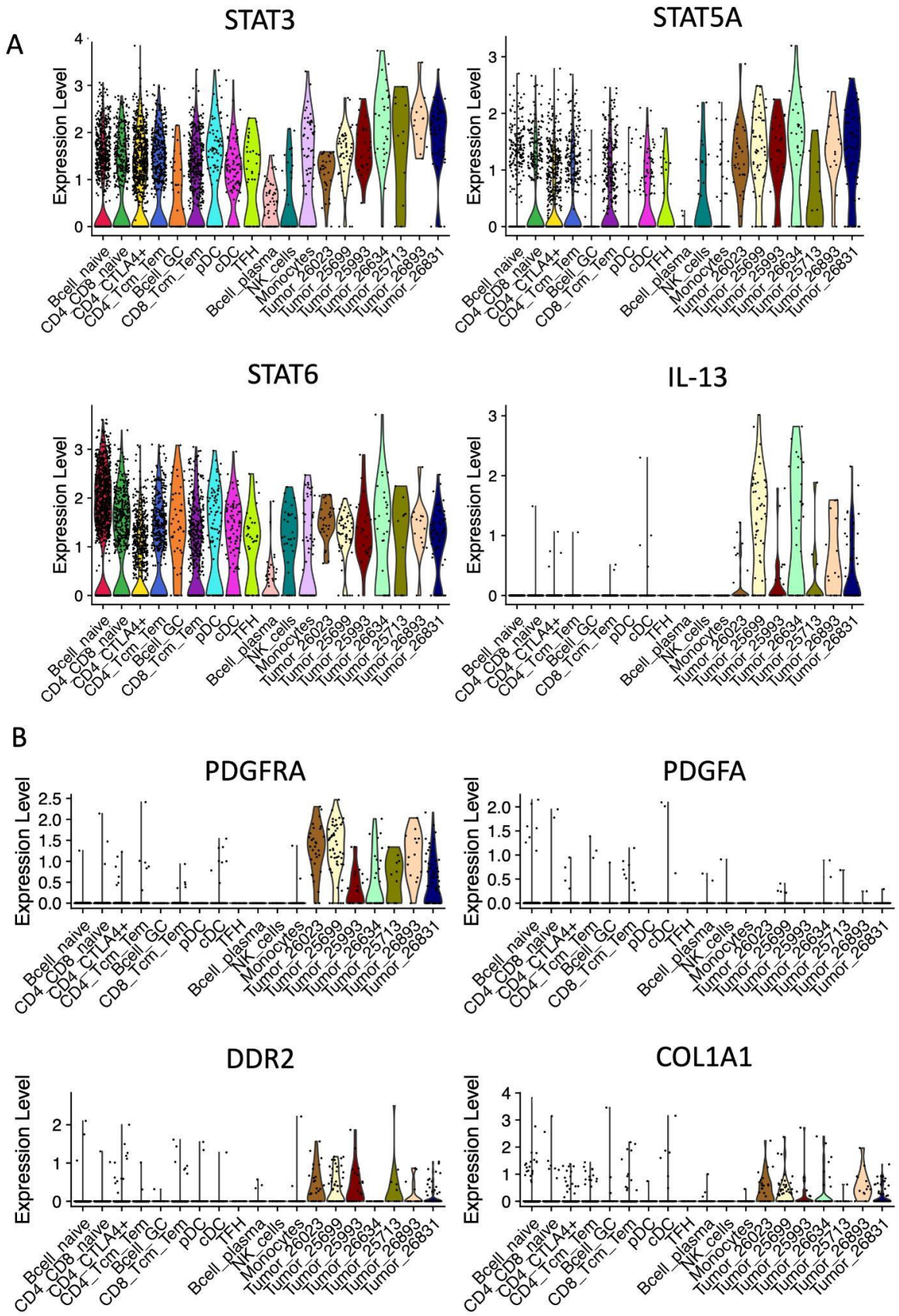

Figure S11 STAT and RTK expression. A) STAT3, STAT5A and STAT6 are highly expressed in HRS cells. IL-13 is also expressed by HRS cells, which can activate STAT6 signalling. **B)** There is variable tyrosine kinase (receptors, (R)TK) expression in patients. PDGFRA and DDR2 are RTKs and PDGFA and COL1A1 their respective ligands.

Table S3. Shaping the HRS TME: cytokines. Cytokine expression and function according to literature, and their expression in the presented data for both HRS cells and the TME. Only cytokines listed in the nine HL TME reference reviews haven been included. If the cytokine receptor was mentioned in the literature their expression is included between brackets after the cytokine expression. V = expressed, X = not expressed. 'Other cell type' indicates that the in literature described cell type was not identified in the presented dataset. 'N/A' implies that there was no information regarding the cytokine expression in either literature or the dataset. Gene names have been used to name the cytokines.

Cytokine	Literature: Expressed in HRS	Data: expressed in HRS	25713	25699	25993	26023	26634	26831	26893	Expressed in TME (literature)	Expressed in TME (cell type)	Function
IL-3	no, (IL-3R yes)[31,35,36,38]	yes 1/7, (yes 4/7)	X, X	X, V	X, X	X, V	X, X	V, V	X, V	T-cells	no (yes, pDC)	CD30L, CD40L upreg, HRS prolif
IL-4	yes[30,34,35]	yes 1/7	X	X	X	X	X	V	V	N/A	no	HL milieu inducer
IL-5	yes[30,31,34,35,36]	N/A								T-cells	N/A	Eosinophil attractant + proliferation
IL-6	yes[30,35,37]	yes 6/7	V	V	V	V	V	V	V	other cell types	no	growth factors (for HRS)
IL-7	yes (IL-7R, yes)[31,34,35,36,38]	yes 1/7	X	X	X	X	X	V	V	T-cells	no	growth factor Tregs + HRS proliferation
IL-8	yes[33,35,36,38]	N/A								other cell types	N/A	attract neutrophils
IL-9	yes[30]	yes 2/7	X	V	V	V	X	X	X	N/A	no	HL milieu inducer, growth factor
IL-10	yes[30-35,38]	yes 4/7	V	X	V	X	V	V	V	T/B-cells	no	anti-inflamatory
IL-13	yes (IL-13R, yes)[30-33,35,36,38]	yes 7/7	V, V	V, V	V, X	V, V	V, V	V, X	V, X	some lymphocytes	no (yes cDC)	HRS growth factor
IL-15	yes (IL-15R, yes)[31,35,38]	yes 4/7	X, V	V, V	V, V	V, X	X, V	V, V	V, V	monocytes, DC	yes B-cells	HRS proliferation + anti-apoptosis
IL-21	yes (IL-21R, yes)[35]	no	X, V	X, V	X, V	X, V	X, V	X, V	X, V	N/A	yes lymphocytes, monocytes, cDC	protects against FAS-apotosis
TGF-B	yes[30-33,35,36,38]	yes 7/7	V	V	V	V	V	V	V	T-cells, monocytes	yes lymphocytes, monocytes, DC	anti-inflamatory + growth factor
TNF-A	yes[30,31,35,36,38]	yes 7/7	V	V	V	V	V	V	V	Lymphocytes + other cell types	no	growth factor
CCL3	no, or low[31]	no	X	X	X	X	X	X	X	T/B cells	yes monocytes	HRS proliferation
CCL4	no, or low[31]	yes 1/7	X	X	V	X	X	X	X	T/B cells	yes T-cells, NK cells, monocytes	HRS poriferation
CCL5	yes[30-38]	yes 7/7	V	V	V	V	V	V	V	T/B cells	yes T-cells, NK cells	Treg, Th2, monocyte,macrophage attractant
CCL11	no[31,36,38]	N/A								other cell type	N/A	T-cell attractant
CCL17	yes[30-38]	yes 6/7	V	V	V	V	V	V	V	monocytes + other cell type	yes T-cells, monocytes, cDC	Treg, Th2 attractant
CCL20	yes[31,35,36,38]	no	X	X	X	X	X	X	X	other cell type	no	Treg attractant
CCL22	yes[30-36,38]	yes 6/7	V	V	V	V	V	V	V	no, or low	yes T-cells, monocytes, cDC	Treg, Th2 attractant
CCL28	yes[31,35,36]	yes 1/7	X	X	X	X	X	V	V	TME	no	eosinophils attractant
CCR3	no[30,35]	no	X	X	X	X	X	X	X	T-cells	no	T-cell homing receptors
CCR4	no[33,35]	no	X	X	X	X	X	X	X	T-cells	no	T-cell homing receptors
CXCR4	no[30,35]	yes 6/7	V	V	V	X	X	V	V	T-cells	yes T/B-cells, DC, NK cells	T-cell homing receptors
CCR5	no[30,35]	yes 1/7	X	X	V	X	X	V	V	T-cells	yes T-cells, cDC	T-cell homing receptors
CCR7	no[30]	yes 7/7	V	V	V	V	V	X	V	T-cells	yes T/B-cells, cDC	T-cell homing receptors
LTA	yes[30,31,35,38]	yes 7/7	V	V	V	V	V	V	V	other cell type	yes B-cells	indirectly enhances T-cell reqruitment
APRIL	yes (receptor: BCMA, yes)[31,35,36]	no (no)	X	X	X	X	X	X	X	other cell type	no (yes B-cells)	HRS proliferation
GM-CSF	yes[31,35,36]	yes 1/7	V	X	X	X	X	X	X	activated T/B-cells	no	M2 TAM differentiation
M-CSF	yes[31,37,38]	yes 4/7	X	V	V	V	V	V	X	other cell type	no	monocytes attractant, M2 TAM differentiation
JAG1	yes[31]	no	X	X	X	X	X	X	X	other cell type	no	HRS proliferation
IDO	N/A	no	X	X	X	X	X	X	X	other cell type	yes cDC	Treg, MDSCs attractant
ICAM1	no[30,31,35]	yes 7/7	V	V	V	V	V	V	V	other cell type	monocytes, DC	Tcell reqruitment
VCAM1	no[30,31,35]	yes 4/7	V	V	X	X	X	V	V	TME	no	Tcell reqruitment
E-selectin	no[30,31,35]	N/A								TME	N/A	Tcell reqruitment
VEGF	yes[30,31,35,36]	N/A								lymphocytes + other cell type	N/A	angiogenesis

Table S4. Cell types educated by the HRS cells. In the nine reviews, used as HL TME reference, different cell types that were educated by the HRS cells were described. Most reviews mention the immunosuppressive Treg population and the TAMs, their characteristics have been summarized here. The remaining cell types have been listed.

Cell type	Characteristics
Tumor associated macrophages (TAMs)	express: CD68+[30,31,32,35,38], CD163+[30,31,32,35,38], PD-L1[31,32], IDO[31], CD206[31] induced by: IL-4[30,32], IL-10[31], Il-13[32], MIF[30], M-CSF[31,32], GS-CSF[31] secrete: IL10[31,32], IL-13[31], TGFb[31,32], CCL17/22[31], STAT3/6[31], PGE2[32] reqruited by: CCR2[30] TAMs are associated with angiogenesis[35]
Regulatory T-cells (Tregs)	express: CD4, IL2RA, FOXP3[30,31,34,38], CTLA4[31,32,36], LAG3[32,34], PD-1[33], CCR4[36] induced and maintained by: IL4[31,34], IL5[34], IL6[31], IL7[34,38], IL10[34], IL13[34,36], IL15[31], PGE2[31,35], galectin1[34,35,37,38], MIF[34], TGFb[35], TIMP[35] secrete: IL-10[32,33,38], CD40L[36], galectin1[36], TGFb[36,38], MIF[36] reqruited by: CCL5[30-38], CCL17[30-38], CCL20[31,35,36,38], CCL22[30,36,38], IDO[34], CXCL10[38] promotes proliferation and survival: IL7[36]
Myeloid-derived suppressor cells (MDSCs)	named by review: 32,34
Tumor-associated neutrophils (TANs)	named by review: 32
Lymph node mesenchymal stromal cells (LN-MSCs)	named by review: 35

Table S5. Summary of HRS cell immune escape mechanisms. Summary of the most described mechanisms, based on the nine HL TME reference reviews, with which HRS cells escape apoptosis and immune detection.

Mechanism	Factor
Treg population expansion	TGFB[30-33,35,36,38] IL-10[30-35,38] IL-13[30,31,34,35,36,38]
cytotoxic T-cell inhibition	Galectin-1[31-36,38]
recrute Treg and or TAMs	MIF - CD74[34,36,38] TIMP-1[31,35] PGE2[31,32,33,35]
overexpressed by HRS to escape apoptosis	cFLIP[31,32,35]
overexpressed by HRS to induce apoptosis	FAS-LG[31,32,35,36,37]
expression loss by HRS to evade immune detection	HLA-I[31-38] HLA-II[31-38] NKG2D ligand[31,35]
overexpressed by HRS to protect from cytotoxic effects	HLA-G[31,32,35] HLA-E[31,32,35]

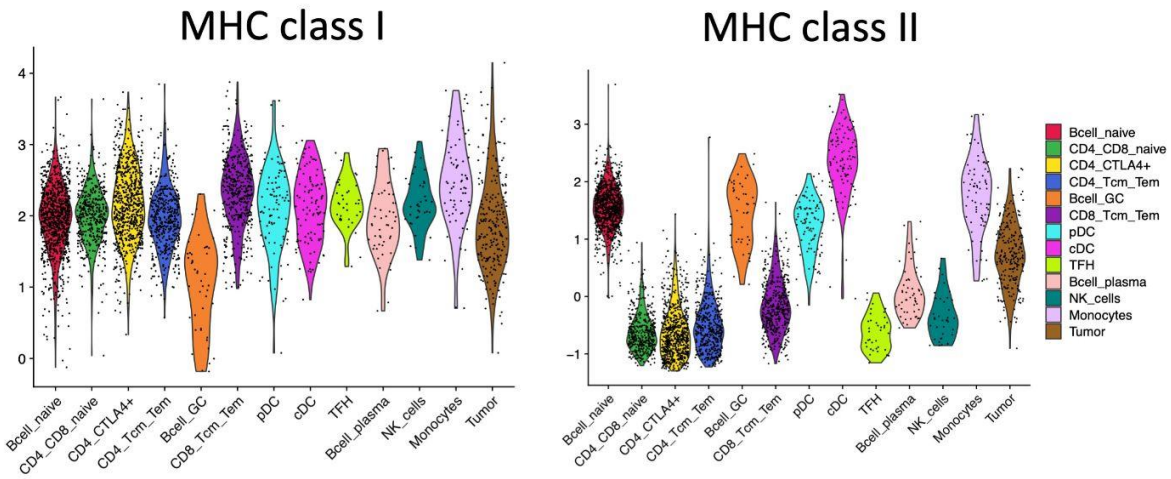

Figure S12 MHC class-I/II expression. Violin plots of each cell type and their corresponding module score. A module score shows the average expression of a given set of markers compared to a random set of markers. MHC-I markers used: HLA-A, HLA-B and HLA-C. MHC-II markers used: HLA-DPA1, HLA-DPB1, HLA-DQA1, HLA-DQB1, HLA-DRA, HLA-DRB1, HLA-DRB5 and HLA-DRB6.

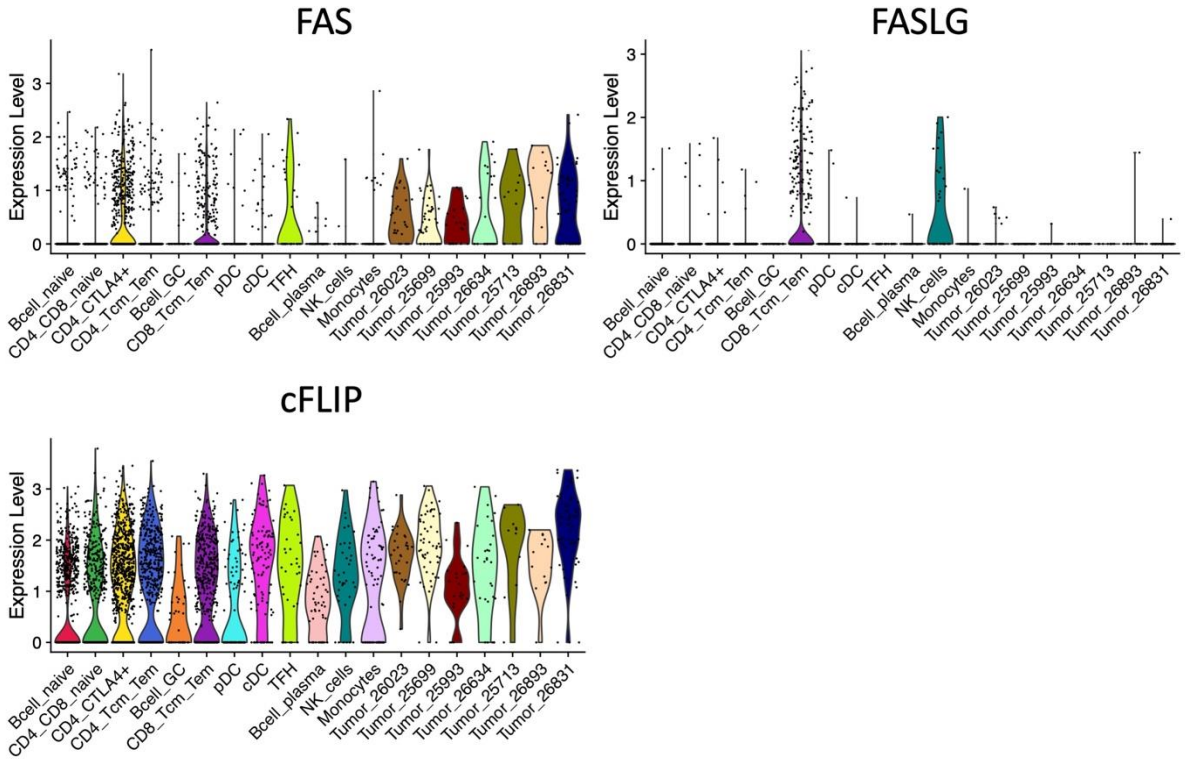

Figure S13 Expression of (anti-)apoptosis markers. FAS ligand (FASLG) can induce apoptosis by binding FAS. cFLIP can inhibit the FAS dependent apoptosis pathway by interfering with the downstream signalling of FAS.